

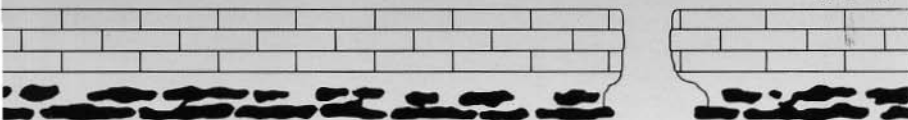
Excursion Guidebook

Marine and Continental Facies with Siliceous Sedimentary Rocks

by

M.A.Bustillo
I.Armenteros
J.A.Blanco

J.Elorza
P.García Garmilla
M.I.Arriortúa



VI INTERNATIONAL FLINT SYMPOSIUM



Excursion Guidebook

Marine and Continental Facies with Siliceous Sedimentary Rocks

by

M.A. Bustillo
I. Armenteros
J.A. Blanco

J. Elorza
P. García Garmilla
M.I. Arriortúa

AGRADECIMIENTOS

La edición de esta guía ha sido posible gracias a las subvenciones recibidas por parte de la Universidad del País Vasco/Euskal Herriko Unibertsitatea y del Instituto Tecnológico Geominero de España.

La Investigación fue realizada a través de los Proyectos de Investigación UPV-130.310E-074-90 y de la C.I.C.Y.T. n.º PB-87-0264

Editor: J. ELORZA, M.A. BUSTILLO Y OTROS

Impresión: GRAFINORTE

ISBN: 84-7585-339-0

DL: 2063-91

PRESENTATION

This field trip, organized on the occasion of the VI International Flint Symposium held in Spain, has as its aim to show a great diversity of sedimentary siliceous rocks in this country. There is diversity not only in the composition but also in the environment where they were formed and their genesis. The itinerary is thus long and is not developed within a single geological context.

The two parts into which this guide is divided correspond to the two large scenes (marine and continental) where the siliceous rocks appeared. Siliceous rocks from a marine environment are analyzed in the Basque-Cantabrian Basin, where the source of organic silica was the main determining factor of its genesis and location. In the Duero Basin the local and restricted continental environments determined the inorganic accumulation of silica, giving rise to thick opaline silcretes.

At all the outcrops chosen as field trip stops, the siliceous rocks were formed by replacement processes of sedimentary rocks. The mineralogical, textural and structural characteristics of the final siliceous rock are determined by the characteristic of the host rock which does not behave as only a good «trap» or reservoir for the silica.

Many factors affect the processes that generate silicification; these range from the sedimentary processes that originated the host rock to the position of this host rock within the structure

of the basin. On this trip emphasis has been placed on this set of factors; the siliceous rocks are not considered independently, but are analyzed in their sedimentary, paleogeographic, diagenetic or tectonic context, depending on the case.

I hope that this field trip will be useful for those people interested in acquiring general and direct knowledge of siliceous rocks, from the perspectives of both Archaeology and Geology.

M^a Angeles Bustillo

Part I

CHERT IN MARINE ENVIRONMENTS

J. Elorza⁽¹⁾, F. García-Garmilla⁽¹⁾, M.I. Arriortua⁽¹⁾,

M.A. Bustillo⁽²⁾

⁽¹⁾ Departamento de Mineralogía y Petrología. Universidad del País Vasco. Apartado 644, 48080 BILBAO

⁽²⁾ Instituto de Geología (C.S.I.C.). José Gutiérrez Abascal, 2. 28006 MADRID

SUMMARY

INTRODUCTION. THE BASQUE-CANTABRIAN REGION

THE UPPER CRETACEOUS SERIES IN THE BASQUE- CANTABRIAN REGION

CHERT TYPES IN THE UPPER CRETACEOUS SEDIMENTS IN THE BASQUE-CANTABRIAN REGION

DAY 1: BARRIKA

MORNING:

FIRST STOP (1.1): THE PLENTZIA FM. IN THE BARRIKA SECTION

- A) THE BASAL ZONE WITHOUT SILICA
- B) SILICA DEVELOPMENT. TYPES OF SILEX
- C) GEOCHEMISTRY
- D) OXYGEN ISOTOPIC DATA OF THE EARLY AND LATE DIAGENETIC CHERT
- E) SILICA DISAPPEARANCE IN THE FINAL PLENTZIA FM.

CRYSTALLINITY INDEX

PICNIC

AFTERNOON:

SECOND STOP (1.2): THE EIBAR FM.

A) THE OLISTOSTROME: RECOGNITION
AND COMPOSITION

B) SILICIFICATION STRUCTURES AND TY-
PES OF CHERT

C) OXYGEN AND CARBON ISOTOPIC DATA
OF THE PLENTZIA AND EIBAR FMS.

**DAY 2: LATE TURONIAN-LOWER
CONIACIAN CARBONATE PLATFORMS IN
NORTHERN BURGOS**

THE HORNILLALATORRE, CUEVA AND
NIDAGUILA FMS.

MORNING:

FIRST STOP (2.1.): THE CUEVA SECTION

A) SEQUENTIAL ANALYSIS

B) SILICIFICATION

SECOND STOP (2.2): THE BEDON SECTION

A) SEQUENTIAL ANALYSIS

B) SILICIFICATION

LUNCH: LOS ROBLES RESTAURANT

AFTERNOON:

THIRD STOP (2.3): THE EL RIBERO SECTION

A) SEQUENTIAL ANALYSIS

B) SILICIFICATION, DOLOMITIZATION AND
CALCITIZATION

ISOTOPIC DATA

**DAY 3: THE PLATFORM MARGIN AND THE
TRANSITION TO BASINAL
ENVIRONMENTS**

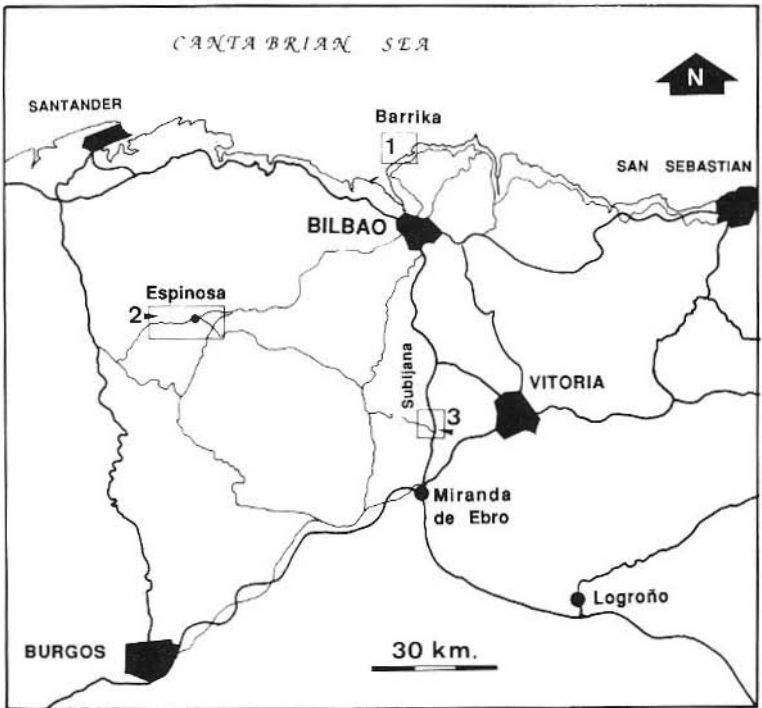
THE VALLE DE MENA, RIBERA ALTA AND LOSAS
FMS.

MORNING:

FIRST STOP (3.1): THE RIBERA ALTA FM. IN THE
SUBIJANA SECTION

A) GENERAL LANDSCAPE AND
SEQUENTIAL ANALYSIS

B) SILICIFICATION



INTRODUCTION. THE BASQUE-CANTABRIAN REGION

The so-called "Basque-Cantabrian Region" or "Basque-Cantabrian Basin" (Northern Spain) comprises a relatively narrow geological setting including most of the Basque Country and Cantabria, the northernmost regions of the Palencia and Burgos provinces and a considerable part of Navarra. The Mesozoic- Cenozoic sedimentary pile is limited by Paleozoic massifs: the Asturian massif to the west, the Cinco Villas massif (Western Pyrenees) to the east and the Demanda massif to the south (**fig.0.1**). The Basque- Cantabrian Region has been divided into four domains according to stratigraphic, paleogeographic and/or structural criteria (**Feuillée et Rat, 1971**): Peri-Asturian (PA in **fig.0.1**), Navarro-Cantabrian which include the Navarro-Cantabrian Trough (NC) and the Northern-Castilian Platform (PN) subdomains, the Basque Arc (AV) and the Ebro Block (BE). The PA, NC, PN and BE domains form the more stable hinterland.

The composite sedimentary series has a thickness of up to 15,000 meters and was deposited as a result of a very prolonged tectono-depositional history from the Triassic period to the Recent. Particularly during the upper Jurassic to the lower Cretaceous, the Region suffered from very important extensional regimes which led to the formation of fault- limited basins related to the continental margin of Northern Spain. The sedimentary record of these basins was of a very varied nature: terrigenous, carbonates, evaporites, vulcanoclastics, etc. (**Soler y José, 1971; Campos, 1979; Pujalte, 1982**).

During the Aptian-Albian an important acceleration of the subsidence rate took place resulting in the progressive marine floodings and the establishment of very shallow seas in which the rudistid carbonate platforms and coral reefs were well-developed. On the other hand, the tectonic movements created flysch troughs in the Basque Arc domain (AV in **fig.0.1**), with the subsequent turbiditic deposits corresponding to the upper Albian-lower Cenomanian (**Rat, 1982, 1983; Badillo and García-Garmilla, 1985**).

An important marine transgression associated with an extensive anoxic episode took place during the Cenomanian-Turonian limit (OAE 3, **Jenkyns, 1980; Renard, 1987**) and was succeeded by several eustatic changes well-represented in the sedimentary record by shallowing-upwards depositional sequences and extensive, widespread carbonate

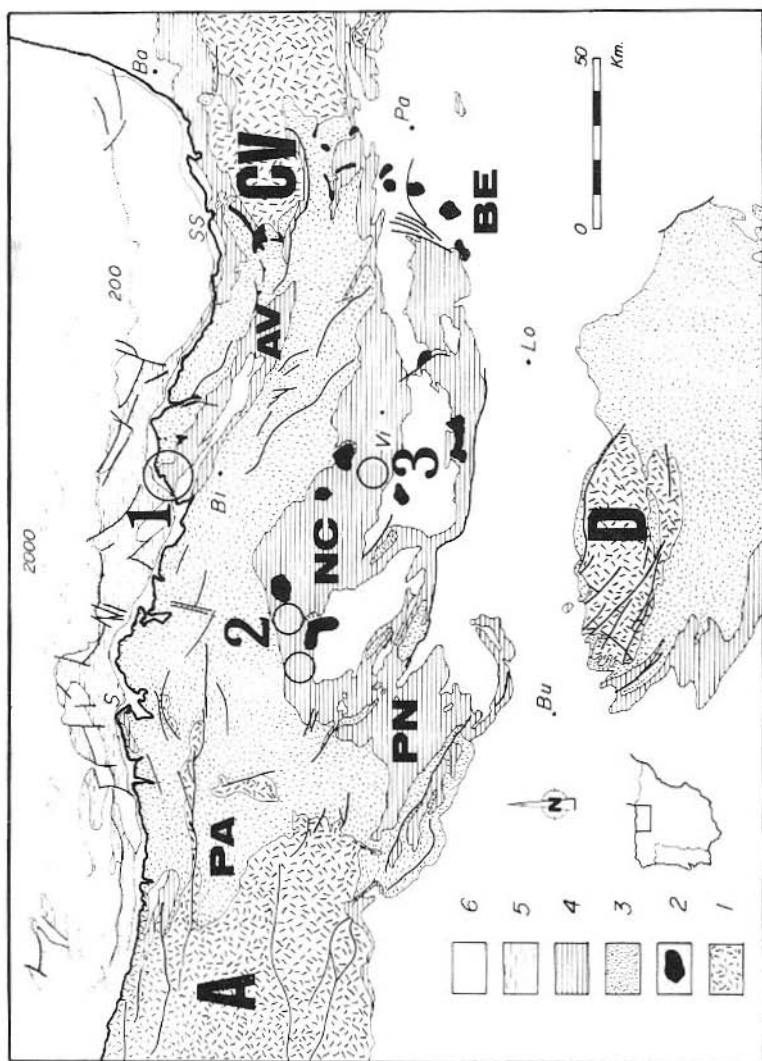


Fig.0.1.- Geological map of the Basque-Cantabrian Region indicating the areas visited during the three days of excursion (1, 2 and 3). In the legend: 1: Paleozoic and lower Triassic; 2: Keuper; 3: Jurassic and lower Cretaceous; 4: upper Cretaceous; 5: offshore Cretaceous; 6: Tertiary and Recent. S: Santander (Cantabria); Bi: Bilbao; SS: San Sebastián; Ba: Baiona; Vi: Vitoria; Pa: Pamplona; Bu: Burgos; Lo: Logroño. PA: Peri-Asturian domain; PN: Northern-Castilian platform; NC: Navarro-Cantabrian trough; AV: Basque Arc; BE: Ebro Block.

platforms in the hinterland domains. Some of them, specifically the upper Turonian-lower Coniacian platforms in the Navarro-Cantabrian domain (NC,PN in **fig.0.1**) include siliceous indicators of shallow marine environments and sedimentary gaps (or sequence boundaries).

On the other hand, the upper Cretaceous series in the Basque Arc are represented by carbonate and sandy flysch successions. Particularly in the Barrika section, as we will see, several horizons bearing nodular chert can be observed associated to turbidite normal-graded beds.

From the late Cretaceous to the upper Eocene, a general episode of compressive phases took place. As a result of this phenomenon, the north-Iberian margin was strongly deformed and folded and the presently observable major tectonic structures were produced (**Boillot, 1981, 1984a,b, fig.0.2**). Nevertheless, other researchers (**Choukroune et al, 1973, fig.0.3**) proposed a strike-slip model, assuming that the north-Pyrenean area was the axis of sinistral strike-slip motions. This mechanism probably could be responsible for the formation of subsident troughs parallelly aligned to the fault zone.

Several authors have carried out extensive reviews about this subject with different hypothesis and conclusions (**Le Pichon et al., 1971; Williams, 1975; Ries, 1978; Deregnacourt and Boillot, 1982**). Moreover, the different types of Triassic and upper Cretaceous vulcanism and their relationships with tectonic factors have been recently studied by **Rosy (1988)**. This work also includes a suggestive review of previous works on the age, temperature, geochemical composition and petrological aspects of the alkaline magmatic events in the Basque-Cantabrian Region.

THE UPPER CRETACEOUS SERIES IN THE BASQUE-CANTABRIAN REGION

The upper Cretaceous sediments show features very different from the Basque Arc to the Navarro-Cantabrian domain (**fig.0.1**). In fact, the paleogeographical, faciological and sequential arrangements differ considerably from the two tecto-sedimentary domains. Specifically, the upper Cretaceous carbonate pile in the Navarro-Cantabrian domain (NC and PN in **fig.0.1**) can be divided into depositional megasequences limited by well-marked sequence boundaries, as defined by **Floquet**

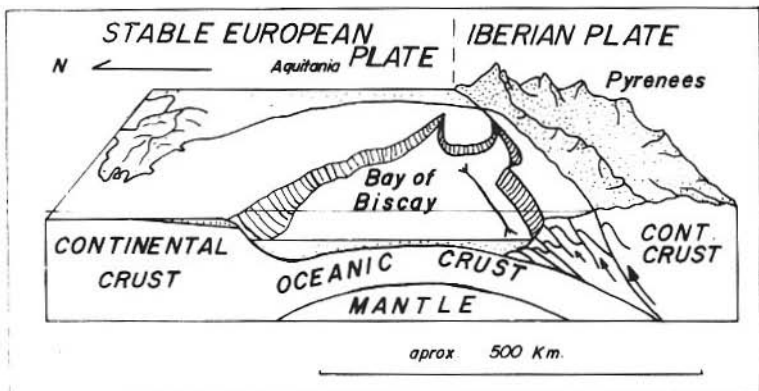


Fig.0.2.- Schematic structure of the Bay of Biscay. Morphology and structure are explained by early Tertiary subduction in the North-Iberian margin (after Boillot, 1984a, b).

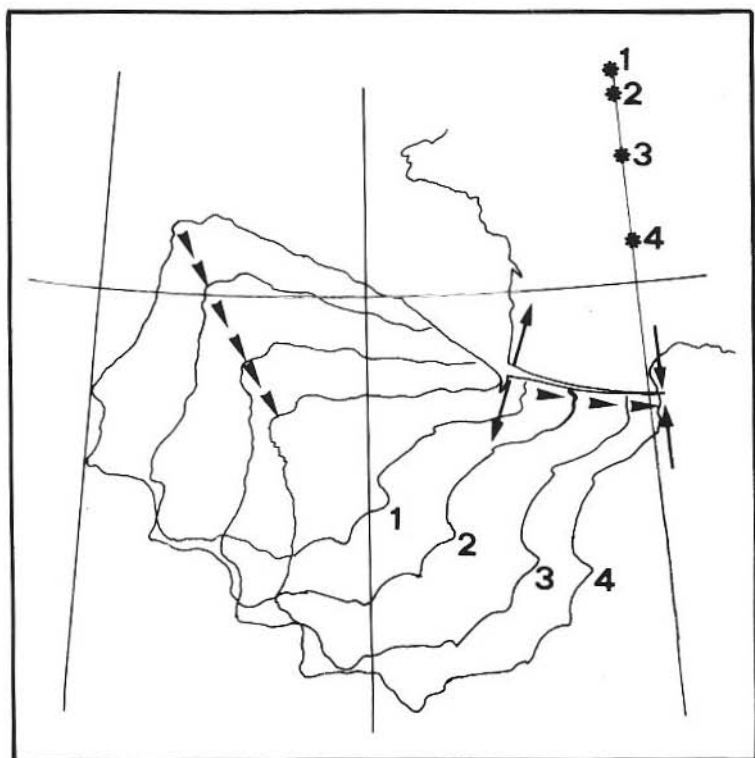


Fig.0.3.- Interpretative schemes proposed by Choukroune et al. (1973). This figure illustrates the Mesozoic displacement of the Iberian Plate around a pole of rotation occupying successive positions (1-4) in a considerable sinistral shifting.

(1983). The limit between the Utrillas sands (upper Albian-lower Cenomanian) and the establishment of the Northern-Castilian carbonate platform is considered by this author as the "crisis" of the middle to upper Cenomanian. Another crisis took place around the late Turonian-early Coniacian, which constitutes the subject of this field-trip (shallowing-upwards megasequence). The middle to upper Coniacian is represented by deeper deposits and the shallowing tendency crows the third megasequence around the late Santonian ("crisis" of the late Santonian, **Floquet**, op.cit.). Finally, the upper Cretaceous last megasequence is marked by a better representation of terrigenous deposits and leads to the continental environments of the early Tertiary ("Garumnian" facies, émersion fini-Crétacé by **Floquet**, op.cit.).

The upper Cretaceous Fms. in the Basque Arc are indicative of deeper environments; for that reason, the recognition and characterization of limit sequences must be looked for accurately. Nevertheless, **Amiot et al. (1983)** have made a first attempt to correlate the crisis mentioned above with the proximal and distal platforms and with deeper marine domains. Thus, the first crisis is marked by the so-called "Black Flysch" (**Rat, 1959; Badillo y García-Garmilla, 1989a,b**) together with the first volcanic manifestations. The second crisis coincides with the establishment of the «Flysch Trough» bearing calcareous deposits. The third crisis corresponds to the enlargement of the "Flysch Trough" towards the ESE and, finally, the fourth one is recorded by the sandy flysch deposition (Eibar Fm.). In the area we will visit on the first day, the erosional and truncation surfaces, the olistostromes and the changes in the paleocurrent models are good markers for delimiting several megasequences. These and other related subjects will be analyzed in the following pages.

Also, the penecontemporaneous tectonic activity could clearly control the subdivision in several sedimentary settings. A very complete scheme by **Floquet (1991)** illustrates the relationship between the carbonate and turbiditic sedimentation and the deep tectonic accidents which determine the different tecto-sedimentary domains in a transversal section from SW to NE (**fig.0.4**). In addition to this type of work, other researchers have focussed their efforts on more local tectonic aspects (**Cuevas et al., 1982; Elorza et al., 1984**).

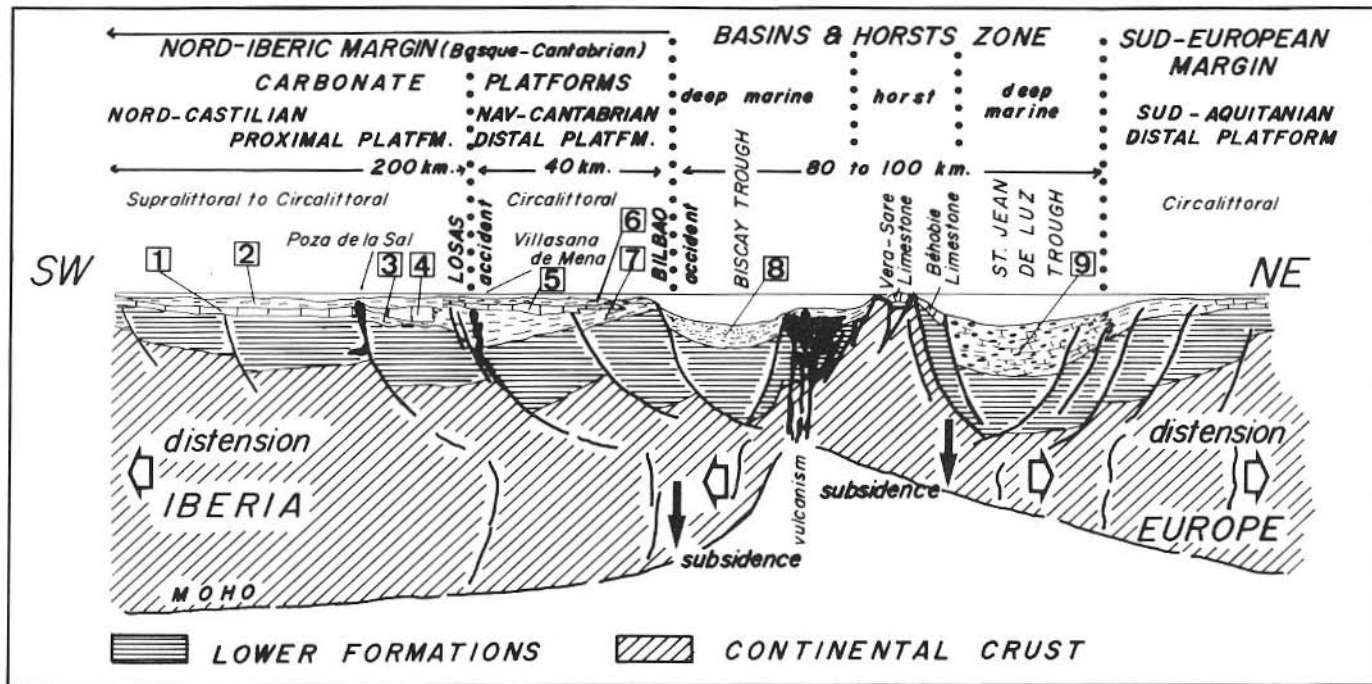


Fig.0.4.- The visited Formations in the different tecto-sedimentary domains along a cross-section of the Basque-Cantabrian Region from SW to NE. The diapirc halokynetic movements are marked just in the Poza de la Sal and Villasana de Mena positions (black-colored). The volcanism in the Biscay Trough (or Plentzia Trough) is also black-coloured. The horizontal hollow arrows indicate the distensional movements, whereas the vertical black ones mark the areas of greater subsidence. 1: Villaescusa de las Torres Fm.; 2: Nidáguila Fm.; 3: Hornillatorre Fm.; 4: Cueva Fm.; 5: Ribera Alta Fm.; 6: Losas Fm.; 7: Valle de Mena Fm.; 8: Plentzia Fm.; 9: Calcareous Flysch with chert. (Modified from Floquet, 1991).

CHERT TYPES IN THE UPPER CRETACEOUS SEDIMENTS IN THE BASQUE-CANTABRIAN REGION

The siliceous manifestations in the upper Cretaceous of the Basque-Cantabrian Region that have been studied so far, can be predominantly found in carbonate Fms. which are considered as belonging to different depositional environments. The selective silicifications on previous anhydrite nodules are particularly interesting, whereas those on bivalves, corals, sponges, echinoids and other fossil invertebrates are less important but still worth-studying.

The development of a very relevant silicification stage showing different features depending on sedimentary environments can be observed in the Basque Arc, Navarro-Cantabrian Trough and Northern-Castilian Platform domains, particularly during the upper Turonian-lower Coniacian interval. This lapse coincides with the maximum degree of silicification in the English Chalk and other European domains, as pointed out by **Mortimore and Wood (1986)**.

A notable silicification has been detected in the Biscay (Plentzia) and St. Jean de Luz troughs (Basque Arc, **figs.0.1 and 0.4**). In regard to the Plentzia Fm., the most significant outcrops that bear chert are located along the coastal zone near the Barrika village. Here, an 800 m. thick carbonate turbiditic sedimentary pile develops. According to **Mathey (1987)**, the Plentzia Fm. was probably deposited in a middle-ocean fan along the so-called «Plentzia Trough». An early silicification begins towards the middle part of the Fm. It appears as continuous bundles which carefully respect the primary sedimentary structures (Tb, Tc, Td turbidite facies). The nodular and bedded cherts are primarily formed by the replacement of carbonate sediments containing less than 50 % of biogenic silica. We employ the term «bedded chert» in a sense different from that of **Maliva and Siever (1989)**. These authors consider the «bedded chert» as primarily formed from recrystallization of siliceous oozes.

A later silicification stage develops at the upper part of the Plentzia Fm. It occurs after irregular fractures from millimeters to few centimeters in size. This silicification is replacing the carbonate material from the fracture surface towards the host rock. Finally, as a result of a very late —and rather hard to date— breaking stage which included associated breccias, a millimetrical infilling of the fractures

is produced. The infilling consists of a thin milky-white-to-bluish patina that bears a conspicuous opaline content.

The Plentzia Fm. is directly overlaid by the Eibar Fm. (800-1000 m., Santonian-upper Campanian), which is composed by siliciclastic turbiditic deposits. An important olistostrome is located more or less near the Santonian-Campanian limit. The olistostrome includes in its basal part large boulders of carbonate turbidites containing early chert. A reactivation of the silicification is clearly observable: a later silicification is associated with the seating fractures of the olistostrome boulders. Since this process results from the dynamic interaction with early chert, it is very interesting to observe the relationship between the two siliceous phases.

In the Navarro-Cantabrian Trough, a very widespread carbonate platform is represented by the Ribera Alta Fm. It includes nodular chert, whose maximum appearance is in the Subijana section, just in the platform sedimentary margin setting. The chert appears as kidney-shaped nodules which are closely controlled by selective silicification processes in the bioturbation networks (*Thalassinoides*).

Since the *Thalassinoides* burrows mark the original bedding planes, the nodular chert appears in the outcrops as non-continuous boudin-shaped bundles. Subvertical bioturbations which are not longer than 20 cm. are occasionally found. The most common host rock for the nodular chert is a bioclastic limestone which is strongly dolomitized in some places. As we will see later on, the dolomitization took place some time after silicification. The silica nodules can reach up to 25 cm. in diameter and appear as individual nodules or continuously-associated rosary-like boudins. Many of their cross-sections show Liesegang rings and a strong dissolution of the carbonate remains in the outermost part of the nodules.

Another type of selective silicification is produced on corals, oysters and inoceramids and consists of different varieties of quartzine-lutecite, megaquartz, etc. In addition, there are small-sized silicified anhydrite nodules containing evaporitic relics which are important paleogeographic markers in the Ribera Alta Fm.

In the Northern-Castilian platform, the Cueva Fm. shows the main amounts of silica in this area. Silica appears here as variable-sized nodular chert always associated with the shallowest facies in the Cueva and Bedón Mountain sections. Similarly, the shallowing trend was

caused by diapiric effects (Salinas de Rosío diapir). Silicification structures have not been observed around the southernmost areas (La Lastra-Sobrón anticlinal area).

Under the microscope, the diagenetic silicification is represented by heavy mosaics of microquartz crystals with lesser fibrous chalcedonite that infill the pores and very abundant siliceous sponge spicule remains and ill-preserved radiolaria (opal A) partially or totally replaced by sparry calcite.

Both spicules and radiolaria suggest a biosiliceous source for the early silica replacing the carbonates. This process could have been dynamic and active during the diagenetic history, and associated with remobilization, silicification and calcitization phases. The calcitization typically occurs along fractures with euhedral crystals included in the microquartz groundmass following the mechanisms proposed by **Maliva and Siever (1988a)** with regard to diagenetic replacements controlled by the force of crystallization.

Although it goes beyond the scope of this field-trip, very interesting silicifications can be detected in the Santonian-Campanian sediments in different places of the Nord-Castilian platform. For instance, near Tubilla del Agua (northern Burgos) the silicification is developed upon anhydrite nodules and it originates the so-called cauliflower-type quartz geodes (**Elorza and Rodríguez-Lázaro, 1984a**). In Langre (Cantabria), there are quartz geodes infilled by celestite (**Elorza and Rodríguez-Lázaro, 1986**), with very contrasted isotopic data for the sulphur values of the celestite (**Boyce et al., 1990**). In the Losa valley (San Pantaleón and Hozalla towns, northern Burgos), the fibrous-radial structures of the celestite are replaced by quartzine-lutecite in a very complex diagenetic pattern (**Elorza and Rodríguez-Lázaro, 1984b**). In the upper Campanian of Laño (near Southern Basque Country), a storm-bed bivalve accumulation underwent silicification. The bivalve shells (*Gryphaea*) have been selectively replaced and it is possible to differentiate several stages of silicification in the shell architecture (**Elorza and Orue-Etxebarria, 1985**). Finally, in the continental paleoenvironments of the Utrillas Fm. (upper Albian-lower Cenomanian), one can find silicification processes on conifer fragments which have been studied by **Elorza and Arriortua (1985)**.

DAY 1. BARRIKA

MORNING:

FIRST STOP (1.1): THE PLENTZIA FM. IN THE BARRIKA SECTION

The Plentzia Fm. was located by **Mathey (1982)** in the north limb of the Bizkaia Synclinorium, specifically in the Barrika section (**figs. 1.1 and 1.2**). This unit corresponds to a middle-outer part of a submarine fan in a carbonate turbiditic environmental complex. The stratigraphic series shows a preferential thinning-fining vertical organization (**fig.1.3**). The total thickness is very difficult to estimate, due to the intense folding affecting it, but it seems reasonably close to 800 m. maximum.

The Tb, Tc and Td intervals of Bouma's turbidite sequence of the Plentzia Fm. are mainly composed by calcarenite and calcisiltite rocks. The horizons oscillate from several centimeters to half a meter thick. A thin micritic limestone usually crowns the turbiditic sequence. Whereas the foraminifera are well-represented in the Plentzia Fm. sediments (*Marginotruncana sigali*, *M. coronata*, *M. sinuosa*, *M. cf. renzi*, *Dicarinella cf. primitiva*), the benthic ostracods (*Pontocyprilla*, *Neocythere*, *Rheacythereis*, *Praephacorhabdotus*) are relatively rare in comparison with those found in the upper and lower Fms. This is owed to unfavorable conditions: anoxia and detrital materials. Two populations of paleocurrents are found in the direction SW-S/SW and N-NE respectively. The Fm. is dated from middle Cenomanian to upper Coniacian/early Santonian. (**Mathey, 1987; Zárrega and Rodríguez-Lázaro, 1990**).

The silicification is by far the most relevant diagenetic process in the Plentzia Fm. It begins around the middle part of the Fm. and is widely developed in the calcarenite facies. The thinner calcarenite is towards the top, the less-developed silicification will be at the upper part of the unit. Near the top, the silicification is completely softened in marly horizons bearing plenty of inoceramids and oysters (*Pycnodonte*). The very thin turbidite calcarenite laminae (1-3 cm. thick) show parallel lamination (Td interval) and visible wedging features in an onlapping structure.

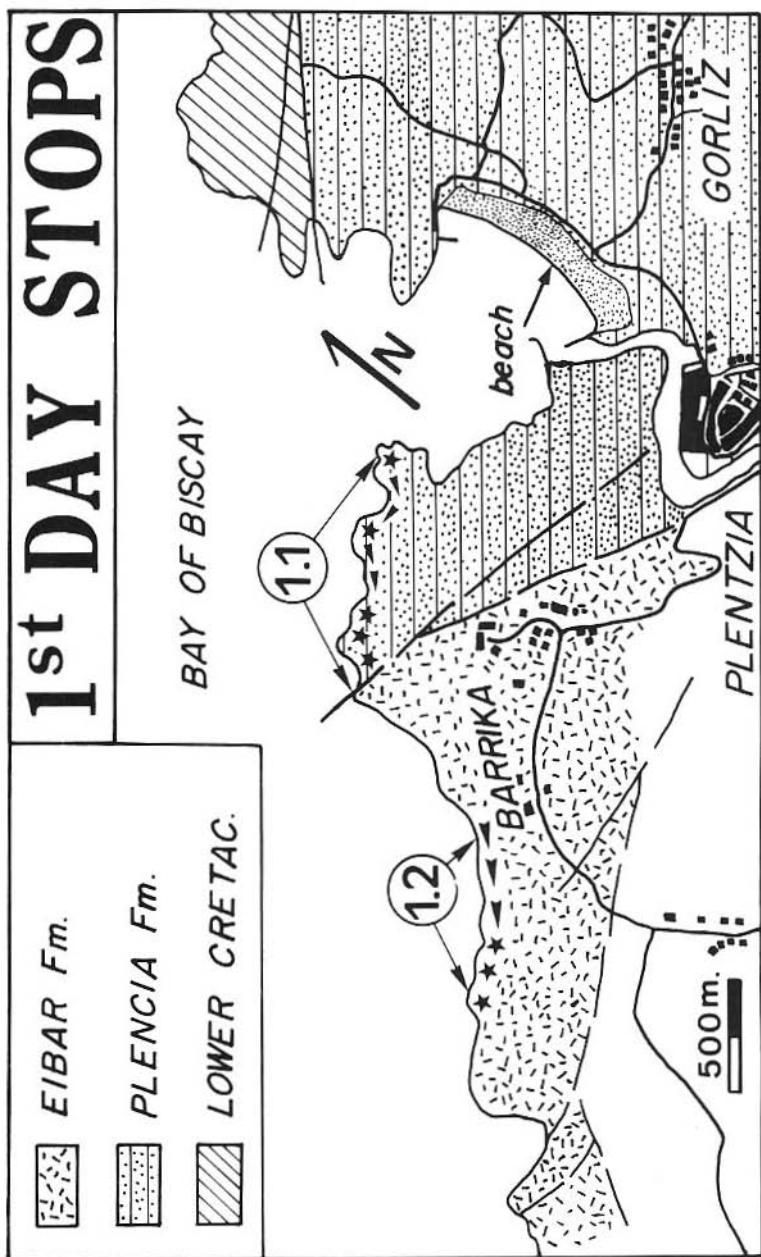


Fig.1.1.- Geographic and geologic location of the itinerary-stops 1.1 and 1.2, and the villages mentioned in the text (North-eastern Bilbao).

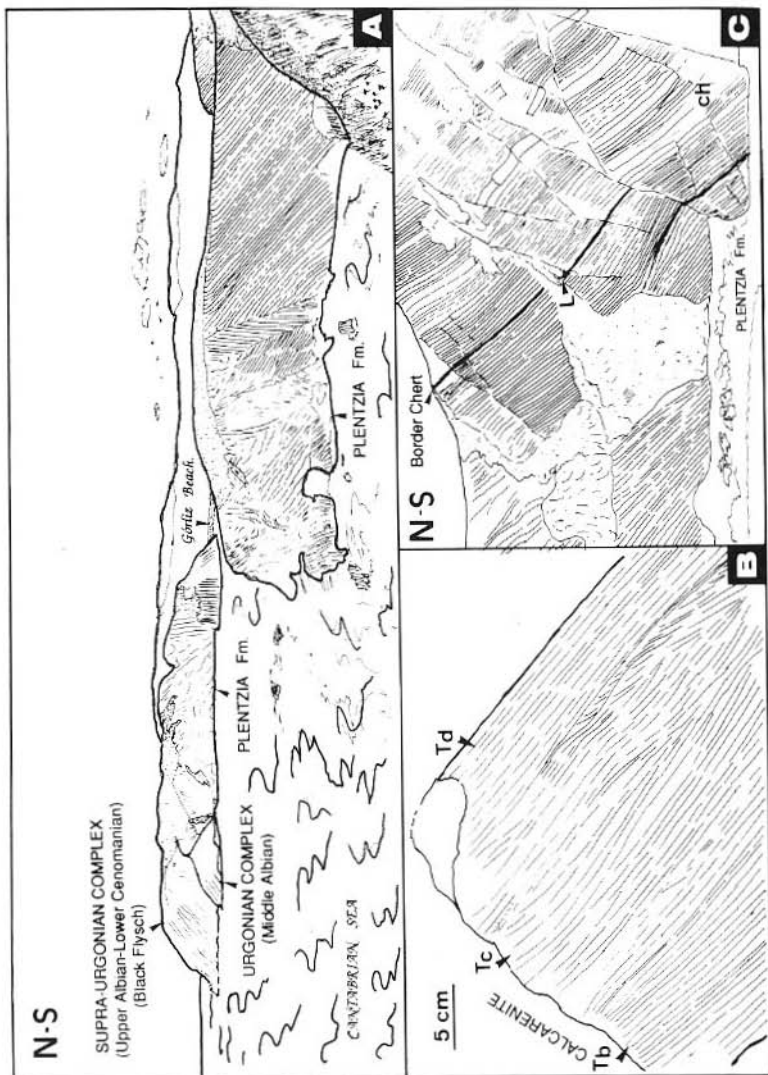


Fig.1.2.A.- A general view of the lower Cretaceous (Urgonian and Supra-urgonian complexes), and the Plentzia Fm. with chevron folds in the Barrika cliffs; **B.-** A detail of carbonate turbidite (Tb-d) without chert in the Barrika cliffs; **C.-** Another general view of the Plentzia Fm. which shows the contact (L) between carbonate turbidites without chert and the beginning of turbidities with chert (ch).

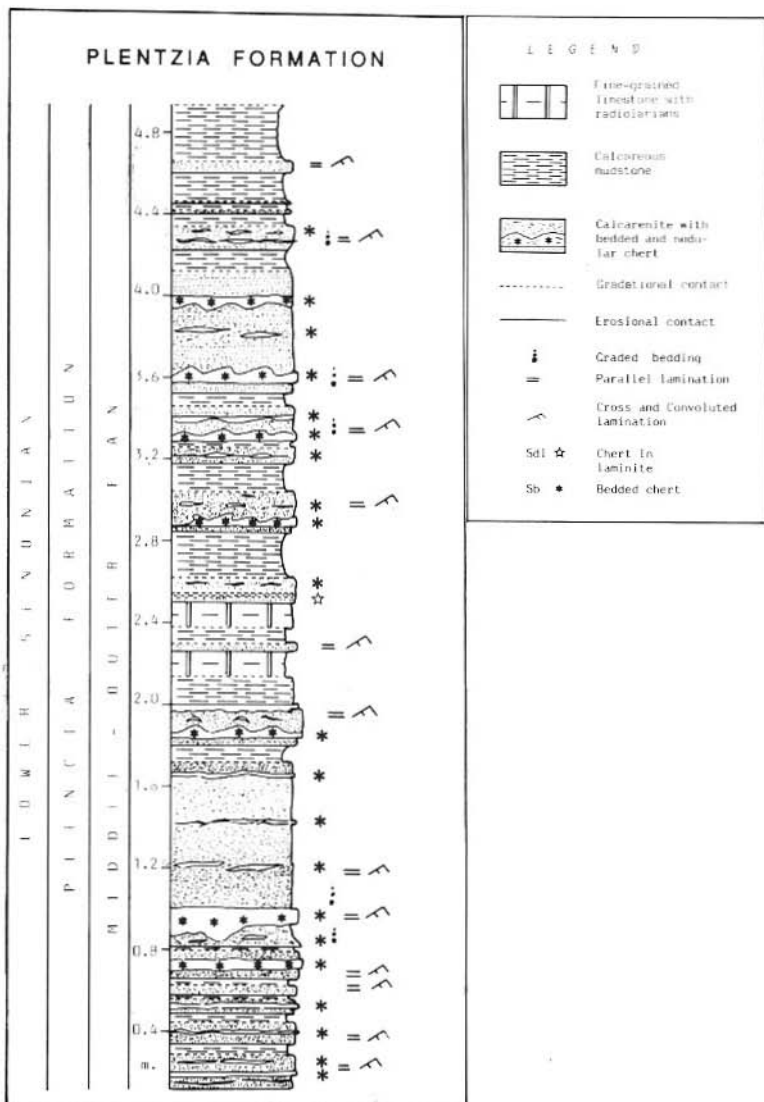


Fig.1.3.- A lithostratigraphic sketch of the Plentzia Fm. with different types of chert in the Barrika (lower Senonian) section. (From Elorza and Bustillo, 1989).

A) THE BASAL ZONE WITHOUT SILICA

The Plentzia Fm. in the Barrika section is composed by carbonate turbiditic beds probably deposited on a middle fan which evolved to an outer one around the final depositional history of the unit. Therefore the silica is absent in the lower and middle Plentzia Fm. The lateral continuity and tabular shape of the beds are not unusual.

Nevertheless, in the non-extreme lower part of the unit, some channelized morphologies can be observed (inner fan subenvironment). Some tens of meters above, there is an olistostrome-like horizon which is several meters thick. This olistostrome is overlaid by progressively thicker and frequent marly beds representing an outer to middle fan. The measured paleocurrents head approximately E-W.

A stratigraphic correlation with the equivalent Fms. in the Navarro-Cantabrian domain (2nd day) is presently speculative due to the lack of continuity in the outcrops. However, along the lines of **Van Wagoner et al. (1988)** with regard to the Systems Tracts philosophy, a first attempt of genetic correlation is showed in the **fig.1.4**. A first sea-level fall (sequence boundary 1, SB 1) could be reflected in a progressive increase and thickening of the calcareous turbidite beds. In addition, the earliest appearance of the nodular chert is associated with the first depositional sequence (DS 1) in the Basque Arc as well as the Navarro-Cantabrian domain.

Under the microscope, the calcarenite facies is packstone-grainstone that bears plenty of foraminifera (few of them arenaceous) and ferroan calcite cement. Some micrite can be observed in thin laminae and locally recrystallized to microsparite and sparite. Siliceous sponge remains (presumably the source of silica) cannot be found.

B) SILICA DEVELOPMENT. TYPES OF SILICA.

In comparison with the sediments without silica, the part of the sequence in which the siliceous manifestations appear is characterized by:

a) A different allochemical composition of the sediment. In fact, the deposits that contain silica are grainstone bearing a large proportion of pellets, sponge spicules (up to 60%), and more rarely radiolaria, foraminifer fragments, detrital quartz (less than 20%) and locally K-feldspar, micas, tourmaline, zircon and apatite. The

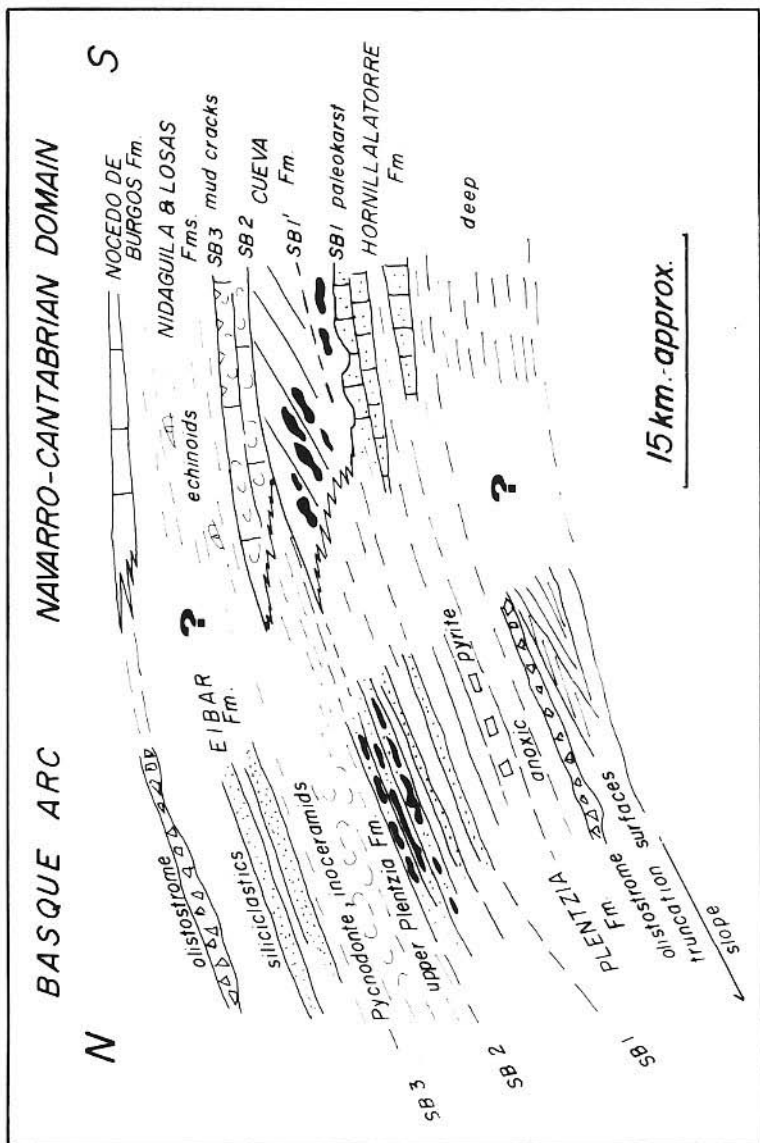


Fig.1.4.- An attempt of correlation -by means of Systems Tracts- between the Fms. belonging to the Turonian-Santonian interval in the Basque Arc and in the Navarro-Cantabrian domain.

argillaceous minerals (less than 10% of the rock) were determined by **Mathey (1987)**.

b) A different direction marked by the measured paleocurrents.

c) Changes in the ostracod associations (increase in diversity).

d) A marly interval indicative of more anoxic conditions (pyrite) is located just below the base of the earliest bearing-chert turbidite bed.

Four types of chert can be distinguished:

- (1) Bedded and nodular chert.
- (2) Chert in poorly-developed laminites.
- (3) Fracture-related chert.
- (4) Chert infilling small fractures.

(1) Bedded and nodular chert.- The bedded and nodular cherts are located in the Tb, Tc and Td intervals of Bouma's turbidite sequence (**fig.1.5,a,b**). The chert nodules range from 2 to 20 cm. thick and the longest dimension is generally parallel to the bedding. The bedded chert contains patches of carbonate representing relicts of the host rock. This type of chert may have a parallel or convolute lamination of the Tb, Td or Tc turbidite intervals kept by the carbonate turbidite replaced by the silica (**fig.1.5**). The morphology of chert nodules is also controlled by primary sedimentary structures of the carbonate turbidite host rocks. Straight boundaries were produced if the host rock had parallel lamination (Tb, Td) and irregular boundaries were produced if the host rock had convolute lamination (Tc interval).

Petrography and Mineralogy. The chert host rock is a calcarenite to coarse-grained calcisiltite that can be classified as grainstone. The most abundant components are siliceous sponge spicules and carbonate pellets (up to 60%); radiolarians, fragments of foraminifers, and detrital quartz are present in minor amounts (< 20%). Siliceous sponge spicules occur in all the carbonate turbidite intervals and define the laminations of Tb, Tc and Td intervals, with a strong decrease in size towards the top of the beds. The cement for the turbidites is chiefly ferroan sparry calcite although microsparite and micrite appear locally. In thicker calcarenite beds (Ta interval), large bioclasts of different nature (orbitolinids, gastropods, coralline algae, echinoid spines, etc) occur together with chert of different nature, polycrystalline quartz and weathered volcanic rock fragments.

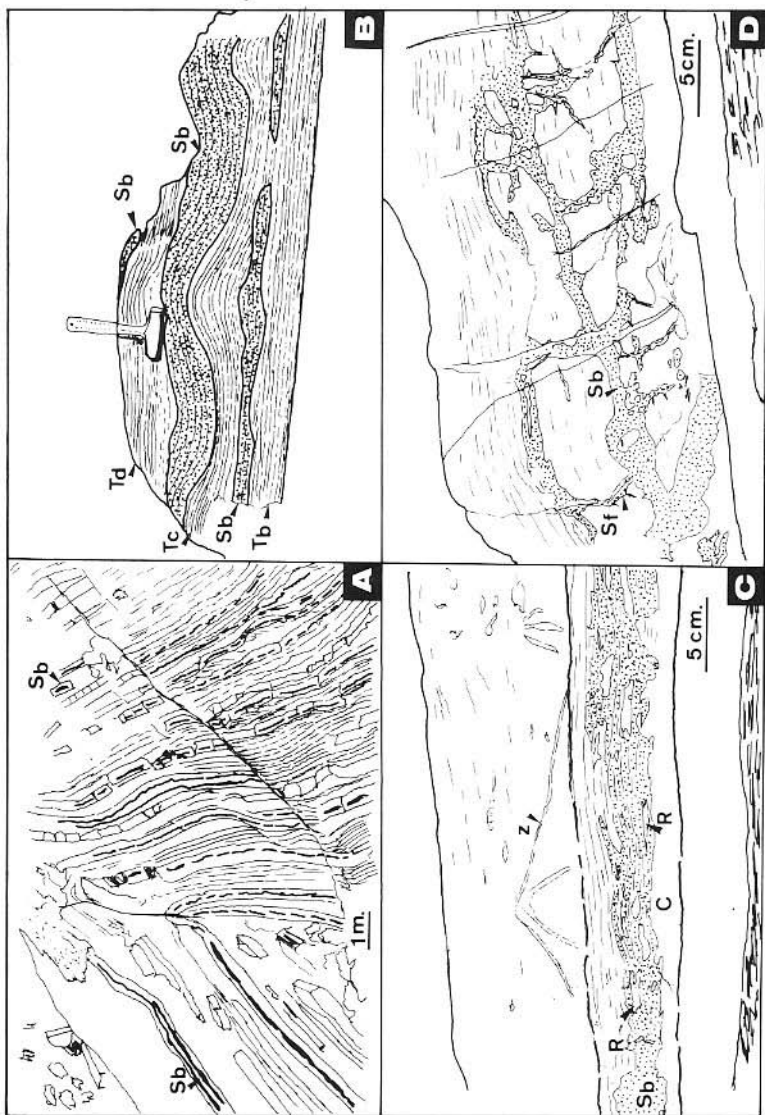


Fig.1.5.- A partial view of the Plentzia Fm. folded with calcarenite turbidite bed and bedded chert (Sb). **B.-** A schematic turbidite bed, belonging to the outcrop 1.1, with bedded chert (Sb) in Tb, Tc, and Td of Bouma's sequence. **C.-** Calcarenite (C) and Bedded chert (Sb) with primary sedimentary structures preserved in the chert. Remains of the host rock (R) that were not silicified occur in the bedded chert. Vertical partial cross-sectional view of a *Zoophycos* specimen (Z) is present. **D.-** Bedded chert (Sb) affected by fractures and forming a later fracture-related chert.

The chert is present only within the calcarenite beds. Most of the silica appears in the form of microquartz and cryptocrystalline quartz, with grain sizes about 20 μm . A fibrous variety of quartz is a minor component. Length-fast chalcedony (chalcedonite) seems to have either replaced the walls of sponge spicules, or to have infilled the axial canals of sponge spicules, radiolarian chambers, and other original sediment voids, or to have replaced some carbonate fossils (foraminifers, bivalves, etc.). Locally, within the sponge spicules, there occurs a brownish-yellow semi-isotropic material considered as an opaline precursor relict phase. Fine-grained iron oxides are also irregularly distributed in the rock.

The source of silica for the formation of bedded and nodular cherts was the dissolution and calcitization of siliceous organisms, mainly sponge spicules and secondarily radiolarians, which were included in the carbonate turbidite beds. The coastal upwelling along the carbonate platform led to a high productivity of siliceous sponges and radiolarians (opal A), which were deposited in the «Flysch Trough» with other allochems as carbonate turbidites. We can see evidence of a maturation process from original biogenic opal A, through an intermediate opal CT composition to microquartz (Maliva and Siever, 1988b).

In its basal part, the Te interval (hemipelagite) is a wackstone. Sometimes a micritic limestone (mudstone) crowns the turbiditic sequence. The limestone is composed of ferroan micrite (mudstone) that contains planktonic foraminifers, radiolarians and sometimes sponge spicules, which are small and always calcified. The clay minerals (illite, smectite, kaolinite and chlorite) range from about 20% to 60% in these intervals (Mathey, 1987).

(2) Chert in poorly-developed laminites.- Chert in poorly-developed laminites consists of thin and poorly-defined alternating chert and limestone (calcarenite) laminae produced by preferential silicification of alternate laminae of the Tb and Td intervals. The silicified laminae range in thickness from several tens of microns to 1 to 2 mm.

Under the microscope, the chert in poorly-developed laminites is predominantly made-up of small spherulites of length slow chalcedonite (quartzine) and smaller amounts of microquartz which are arranged in laminae. The quartzine tends to form aggregates of spherules in all laminae that contain dolomite and iron oxide particles.

The fibrous texture of quartzine was probably formed in an alkaline or sulfate diagenetic microenvironment (**Folk and Pittman, 1971**); also, the precipitation of quartzine may indicate that pore fluids were rich in magnesium and that they were saturated with respect to quartz (**Jacka, 1974; Hatfield, 1975, Folk, 1975; Keene, 1983**).

(3) Fracture-related chert.- Fracture-related chert has irregular, rectilinear, or curved shapes and occasionally cross-cuts the carbonate turbidite beds. This chert can be found at the middle-upper part of the series. The fracture-related chert is never found in the hemipelagite mudstone. The irregular contact with the host rock shows that the silicification is not the simple infilling of an open fracture but is mainly the replacement of the adjacent carbonate rock.

These fractures cross the bedded chert and laminite-hosted chert. The width of the fracture-related chert (from mm. to cm) increases when the fracture passes from the bedded chert to the carbonate host rock. Sometimes the inner part of the fracture is infilled by sparry calcite.

(4) Chert infilling small fractures.- Sometimes the bedded chert contains millimeter-sized fractures filled with white-blue chert. These fractures are local and limited in thickness, with areas of microbrecciation. The silica never replaces the adjacent carbonate host rock or the early microcrystalline chert. Since this type of chert infilling fractures presents a white-blue opaline aspect, it can only be detected inside the early bedded chert. Also, it is difficult to determine their exact formation time.

Microscopically, this late chert has an opaline aspect with at least two generations of silica: a) a brownish-yellow semi-isotropic fibrous chalcedonite, with microbanded laminations. b) a minority fibrous chalcedonite with no inclusions and related to the first generation (**fig. 1.12**).

C) GEOCHEMISTRY

Trace and major element compositions of cherts and trace element composition of grainstones (host rock) were determined by X-ray fluorescence spectroscopy (**Elorza and Bustillo, 1989**). The silica content of the untreated chert ranges from 84 % to 88 %. Untreated cherts contains more Fe and Na than their HCl treated counterpart. Fe and Na oxides are mainly contained in the carbonate

minerals. The other oxides, except silica, either are minor or do not show a consistent behavior (**Table I**).

The contents of Zr, Pb, Rb and Zn are relatively high in the Barrika cherts. These elements are below the limits of detection in the host rock. In untreated chert, Rb, Pb, Th, Zn, Ga? and Zr are less abundant than in HCL-treated chert, which suggests that these trace-elements are not associated with calcite.

No difference exists between the content in minor elements in bedded, nodular, and fracture-related chert, because all of these cherts were formed by the replacement of the host carbonate. Sr and Zr are the most abundant trace-elements; Sr is also associated with the carbonate host rock, but Zr is not. Zr may be incorporated in iron minerals. Pb, Zn and, to a lesser extent, Rb may be included in the hematite (**Table II**). Most of the minor elements detected may appear in association with hematite, which is common in many cherts.

The presence of these geochemical elements can be explained as follows: the silica-rich fluids were also somewhat enriched in minor elements (Zr, Pb, Zn, Pb) as the result of the dissolution of biogenic silica, but primarily of the leaching of the hemipelagite beds, mainly the clay minerals. During early diagenesis, silicification caused the rejection of the minor elements from the chert and their concentration in the calcarenite beds, which had a greater effective porosity than the mudstone beds. Throughout the silicification process, the minor elements were incorporated in the silica-rich solutions from which the initial diagenetic opaline phase was precipitated. Later on, when the diagenetic opaline phase became quartz, the minor elements were probably incorporated into the iron oxides (hematite).

D) OXYGEN ISOTOPIC DATA OF THE EARLY AND LATE DIAGENETIC CHERT.

We assume that $\delta^{18}\text{O}$ in cherts is the latest transition from opal CT to quartz, and not the original precipitation of any siliceous phase from the ocean, as opal A from the sponge spicules. We can see, at least, two possible reasons for the systematic 1‰ difference: a) both types of chert were formed from fluid of identical $\delta^{18}\text{O}$ but at different temperatures; b) both types of chert were formed at the same temperature but from isotopically distinct fluids. We know that the bedded-nodular

TABLE I.- Chemical composition in weight percent of cherts, by X-ray fluorescence spectroscopy.

	N-1	N-3	N-4	N-4*	N-5	N-12	N-12*	NF-1	NF-5
SiO ₂	97.58	98.00	97.30	83.98	97.51	97.65	88.59	98.29	98.15
Al ₂ O ₃	0.16	0.07	0.74	0.37	0.45	0.31	0.30	0.15	0.25
Fe ₂ O ₃	0.26	0.13	0.13	0.48	0.16	0.13	0.59	0.06	0.05
MnO	0.01	0.01	0.01	0.01	0.01	0.01	0.01	0.01	0.01
CaO	1.02	0.80	0.80	7.91	0.80	0.80	5.44	0.81	0.80
Na ₂ O	0.01	—	—	0.21	—	0.01	0.13	—	—
K ₂ O	—	—	—	—	—	—	—	—	—
TiO ₂	0.02	0.02	0.03	0.02	0.04	0.03	0.02	0.02	0.02
Loss on fusion at 1050°C	0.88	0.71	0.80	6.72	0.81	0.77	4.84	0.81	0.85
Total	99.94	99.74	99.81	99.70	99.78	99.71	99.92	100.15	100.13

Key: N, HCl-insoluble residues of nodular and bedded chert. N*, bulk untreated chert. NF, chert related to fractures (total iron as Fe₂O₃).

TABLE II.- Trace elements composition of roks, in parts per million.

	Rb	Ba	Pb	Sr	Ce	Y	Th	Zn	Cu	Ni	Ga	Zr
Bedded and nodular chert, HCl-treated												
N-1	64	7	38	180	10	23	25	34	11	7	24	165
N-2	69	—	35	177	9	26	28	51	10	7	25	185
N-3	72	8	39	182	9	26	27	45	11	7	26	181
N-4	69	23	37	185	9	25	28	61	12	8	26	180
N-4*	51	—	28	291	10	20	21	23	9	7	21	131
N-5	70	18	38	181	9	25	28	38	10	6	26	181
N-6	73	12	37	182	9	26	28	38	11	8	25	182
N-7	70	—	36	179	10	26	29	40	10	9	25	182
N-8	70	—	38	182	9	26	28	39	10	7	24	181
N-9	71	7	37	181	9	26	28	47	10	7	26	184
N-10	69	16	35	183	9	26	30	47	11	7	24	185
N-11	71	—	39	181	9	25	26	44	10	7	25	182
N-12	69	—	39	181	9	22	27	41	10	7	24	184
N-12*	55	10	33	251	8	22	22	27	12	9	22	145
Fracture-related chert, HCl-treated												
NF-1	69	—	37	186	9	25	27	54	12	7	25	178
NF-2	69	—	37	192	8	26	28	48	10	6	25	181
NF-3	69	—	38	90	8	26	27	45	9	7	25	184
NF-4	70	—	39	184	8	26	28	34	9	7	24	178
NF-5	70	—	35	188	9	26	28	39	11	6	24	186
Calcarenites												
LF-29	17	—	6	410	8	7	—	—	8	—	13	26
LF-30	—	—	6	390	8	—	—	—	8	—	11	—
LF-32	—	—	—	379	8	—	—	—	—	—	11	—
LF-36	—	—	—	361	8	—	—	—	8	—	11	—
LF-48	—	—	7	326	8	—	—	—	7	—	12	19
LF-61	—	—	—	438	8	—	—	—	7	—	13	12

Key: —, less than 5 ppm. *Untreated sample.

chert is formed in the Plentzia Fm. (carbonate turbidites of Coniacian age) and the later fracture-related chert is found within big fragments of the Eibar Fm. (sandy flysch of Santonian-Campanian age). The Eibar Fm. was deposited deeper and later than the Plentzia Fm., thus, we suggest that both classes of chert were formed from fluids of similar $\delta^{18}\text{O}$, due to the same composition of their rock, but with different temperatures given the difference in depth between them (**Elorza and Fallick, in press**).

There are several expressions in the literature which suggest a relationship between $\delta^{18}\text{O}$ (H_2O), $\delta^{18}\text{O}$ (SiO_2) and temperature. All of them assume that the silica is formed in isotopic equilibrium with the interstitial fluid. We choose the **Kita et al. (1985)** expression and we can see that 1‰ in $\delta^{18}\text{O}$ (SiO_2) systematic difference corresponds to a 5°C temperature difference (with later fracture-related chert forming at higher temperature). If we assume a depletion of $\delta^{18}\text{O} = 0 \pm 1\%$ relative to the Standard Mean Ocean Water for the oxygen isotopic composition of Cretaceous seawater, we find a diagenetic temperature of 45 to 55 °C.

E) SILICA DISAPPEARANCE IN THE FINAL PLENTZIA FM.

The Plentzia Fm. vertically evolves to a gradual diminution in carbonate turbidites which implies a subsequent increase in the marly terms. The turbidites only consist of parallel-laminated thin beds or laminae (1-3 cm. thick) and some of them are wedge-shaped. Chert can be most commonly found in very thin laminae following the primary lamination of the rock but, in general, the silica disappears because of the lack of a sufficient amount of sponge spicules. Thus, the siliceous diagenetic processes are extinct.

A large number of non-silicified *Inoceramus* (complete shells and fragments with thick and weak walls) and some small specimens of *Pycnodonte* appear in the marly sediments. They have a notable paleogeographic interest, as will be seen later on.

With regard to the Systems Tracts nomenclature (see **fig.1.4**), the upper marls of the Plentzia Fm. are probably equivalent to the DS 2 depositional sequence identified in the Navarro-Cantabrian domain (2nd day) and perhaps also to the lower Nidáguila and Losas Fms., both Fms. being indicative of a major transgressive episode.

CRYSTALLINITY INDEX.

Following the methods proposed by **Murata and Norman (1976)** and **Gregg et al. (1977)**, **Elorza et al. (1985)** have determined the Crystallinity Index (C.I.) of 20 early bedded chert samples (Barrika section). The parameters and the cell unit volume were determined through the refined least-squares method applied on data obtained by X-ray diffraction.

If we compare the (C.I.) variations — obtained after the application of two methods — with the variations of the cell unit volume, and with the impurity percentage, we do not find the existence of a clear direct relation. However, when we organize the samples in three groups, according to their external aspect, certain tendencies can be observed (**Table III**).

In this way, the (C.I.)'s determined by the method of **Gregg et al. (1977)** decrease when the cell unit volume and the impurities increase, as some other authors have also pointed out (**fig.1.6**). This tendency was confirmed later on by other chert samples of the Basque-Cantabrian Basin (**Arriortua et al. 1984; Elorza y Arriortua, 1985; Tarrío et al. 1989; Urtiaga et al. 1991**).

PICNIC

AFTERNOON:

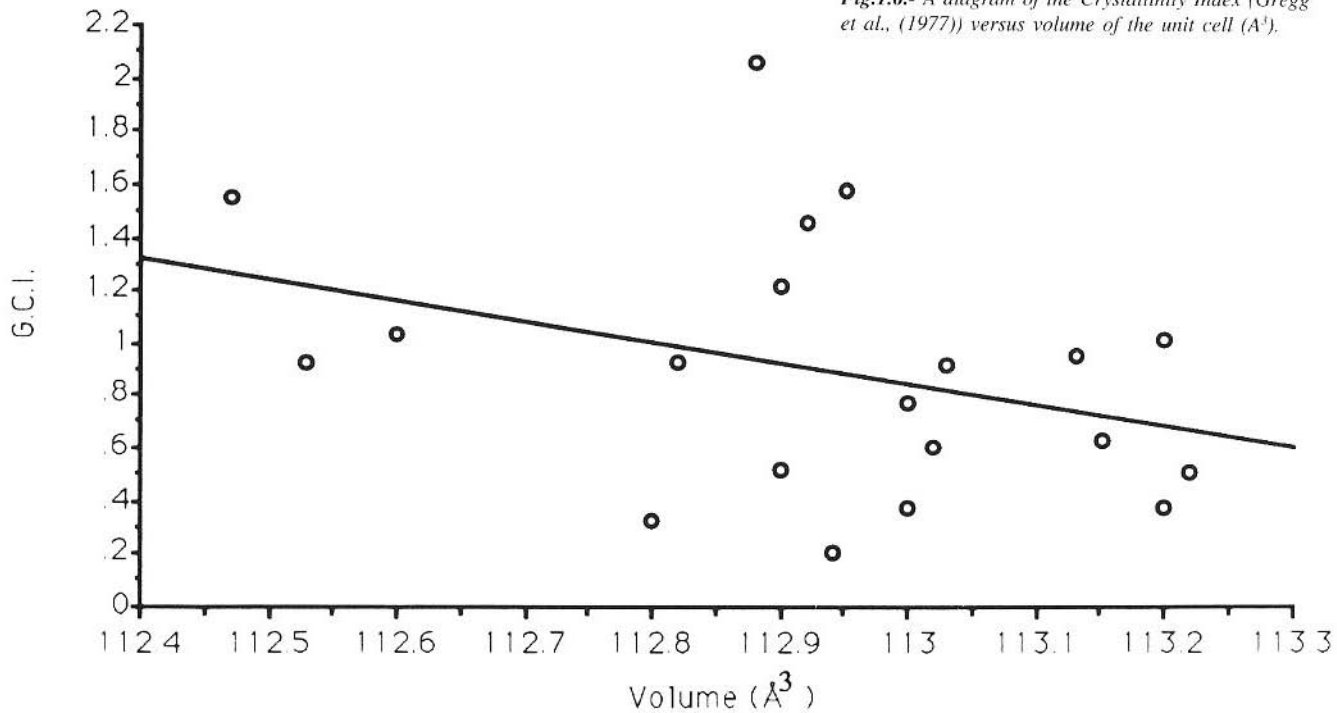
SECOND STOP (1.2): THE EIBAR FM.

The Eibar Fm., identified by **Mathey (1982)**, conformably overlies the Plentzia Fm. It is composed by sandstones or micaceous argilites in alternation with calcareous siltstones or grayish marlstones (sandy flysch). The turbiditic siliciclastic beds have an individual thickness ranging from several centimeters to one meter and frequently show current structures (Tb, Tc and Td intervals) and organic structures in their bases (*Planolites*, *Granularia*, *Helminthopsis*). The Te term is represented by easily-alterable obscure marls bearing pyritized bioturbations. Sometimes the turbidite sequences are crowned by a finely-grained limestone horizon that bears planktonic foraminifera (*Globotruncanidae*, *Heterohelicidae*) which corresponds to a typical hemipelagic sedimentation.

TABLE III.- Volume of the unit cell and crystallinity index (C.I) of the bedded chert that appears in the Barrika section.

Samples	a(A)	c(A)	Volume of the unit cell	(G.C.I.) GREGG et al.	(M.C.I.) MURATA- NORMAN	Impurities %
LF-5	4.907(1)	5.339(1)	112.60(4)	1.03	1.66	0.29
LF-9	4.9176(7)	5.405(1)	113.20(3)	1.01	3.29	0.82
LF-11	4.9163(8)	5.404(1)	113.13(2)	0.95	2.61	0.62
LF-13	4.9107(7)	5.402(1)	112.82(4)	0.93	1.83	0.76
LF-26	4.905(2)	5.399(3)	112.53(8)	0.92	2.24	0.23
LF-34	4.9129(0)	5.403(2)	112.95(4)	1.57	1.75	0.60
LF-69	4.906(2)	5.394(3)	112.47(6)	1.55	2.63	0.18
B	4.911(8)	5.403(1)	112.88(3)	2.05	1.54	0.54
LF-14	4.915(2)	5.404(6)	113.0(1)	0.77	3.55	0.64
LF-28	4.9137(6)	5.4005(9)	112.92(3)	1.45	2.43	0.57
LF-83	4.909(5)	5.412(2)	112.9(3)	1.22	4.73	0.56
LF-7	4.904(1)	5.421(1)	112.9(5)	0.52	5.81	0.56
LF-16	4.912(1)	5.409(2)	113.03(5)	0.91	5.29	0.67
LF-18	4.912(3)	5.398(4)	112.8(1)	0.33	5.94	0.46
LF-24	4.909(2)	5.409(4)	112.94(8)	0.20	6.17	0.59
LF-29	4.914(1)	5.403(1)	113.02(5)	0.60	5.32	0.66
LF-36	4.913(0)	5.419(1)	113.2(1)	0.37	5.40	0.82
LF-61	4.9170(7)	5.404(2)	113.15(5)	0.62	4.53	0.78
LF-71	4.914(3)	5.401(8)	113.0(2)	0.37	5.00	0.64
A'	4.918(1)	5.403(2)	113.22(6)	0.50	4.60	0.85
Quartz	4.9027*	5.3934*	112.27*	1.1(2)*		

*Standard values for quartz from International Union of Crystallography (1963, V. 3, p. 112).



The Eibar Fm. has a total thickness of 1000-1200 m. in the northern limb of the Bizkaia Synclinorium. It was deposited in the so-called «Orio Trough» during the late Santonian-lower Campanian interval and possibly represents a fan-fringe subenvironment. **Fig.1.7** illustrates the lateral and vertical relations between the Fruniz, Plentzia and Eibar Fms. As can be seen, the Plentzia Fm. laterally intertongues with the calcareous Fruniz Fm. which bears volcanic intercalations. The latter fm. is composed by alternating mudstone and limestone beds together with submarine volcanic rocks (lava flows and breccias). The Eibar Fm. conformably overlies the Plentzia Fm. with a slighty diachronic boundary.

A) THE OLISTOSTROME: RECOGNITION AND COMPOSITION

Along the Barrika section, two olistostromes can be identified, as pointed out by **Cuevas et al. (1982)**, **Mathey (1987)**, and **Elorza and Bustillo, (1989)**. The first and lower olistostrome is composed by sandy-flysch boulders together with green volcanic rock fragments, quartz masses and, probably, hydrothermal-in- origin iron oxides with quartz. These components are included in a reddish calcareous-argilitic groundmass. The study of this olistostrome goes beyond the scope of this field trip.

The second olistostrome is not directly located upon the former and has a greater thickness (about 40 m.). Due to the tectonic folding, it outcrops in an inverted position showing a great number of boulders which are very different in composition and age. It is normally-graded from large boulders at the base to a calcarenite episode at the top (**figs. 1.8, 1.9**).

Some considerations about the age of the materials are of interest. The samples obtained from points 1 and 6 in **fig.1.8** (sandy flysch) have the same age (late Santonian). On the other hand, the remaining samples sharply contrast in age. Sample 2 is middle Cenomanian; sample 3 is middle Coniacian; sample 4 is Coniacian and sample 5 has been dated as late Santonian in age. The age determinations were carried out from planktonic foraminiferal species (**Elorza et al., 1987**).

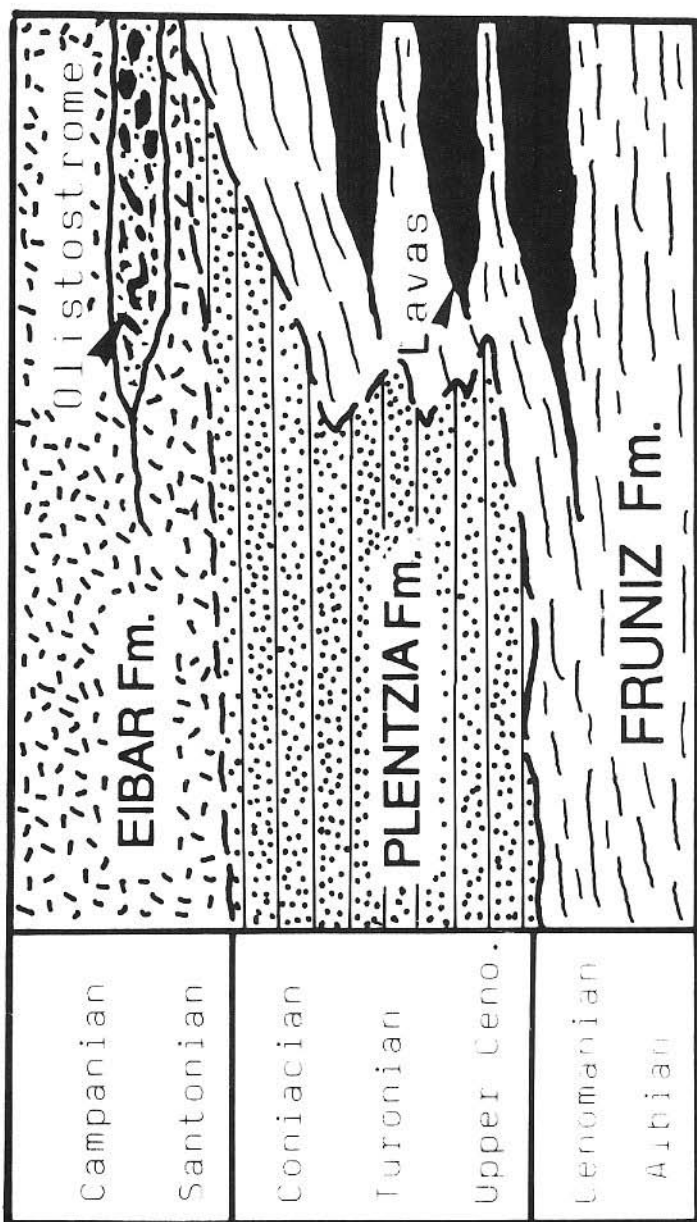


Fig.1.7.- A composite stratigraphic section of the Fruniz, Plentzia and Eibar Fms. (Based on Mathey, 1982).

B) SILICIFICATION STRUCTURES AND TYPES OF CHERT

Large blocks of carbonate turbidite beds, with bedded and nodular chert, belonging to the Plentzia Fm. form part of the olistostrome (**fig. 1.10 A**). These blocks of calcarenite are thicker (1 to 2 m) than the first one discussed above, which suggests a proximal formation setting.

We can see three types of chert:

- 1) bedded and nodular chert,
- 2) chert in poorly developed laminites,
- 3) fracture-related chert.

In general, they present the same characteristics as the types of chert examined above.

(1) Bedded and nodular chert.- The beds and nodules of chert are located in the Tb, Tc and Td intervals of Bouma's turbidite sequence. The bedded chert contains patches of carbonate representing relict host rock when the silica supply was low (**fig. 1.10 B**). The internal structure of the host rock may have determined the location of the nodular chert. Thus, we can see nodules that are mainly established in the anticlinal cores of undulate lamination (Tc interval) (**fig. 1.10 C**), which suggests that silica-rich fluids migrated laterally along the sedimentary structures, and replaced the high-porosity carbonate sediment in favorable places.

The morphology of the bedded chert is controlled by primary sedimentary structures of the carbonate host rock. Straight boundaries were produced in those cases in which the host rock had parallel lamination (Tb, Td) and irregular boundaries were produced if the host rock had convolute lamination (**fig. 1.10 D**). In general, they present the same textures than the bedded and nodular chert examined in samples of the Plentzia Fm. under the microscope.

Only in this outcrop, the tabular and nodular cherts are affected by a specific fracturation and brecciation. This fracturing may have been generated during and after deposition of the olistostrome as a consequence of readjustment of the carbonate turbidite blocks inside the olistostrome. The distance between the chert fragments ranges from millimeters to several centimeters and were rotated in places, whereas

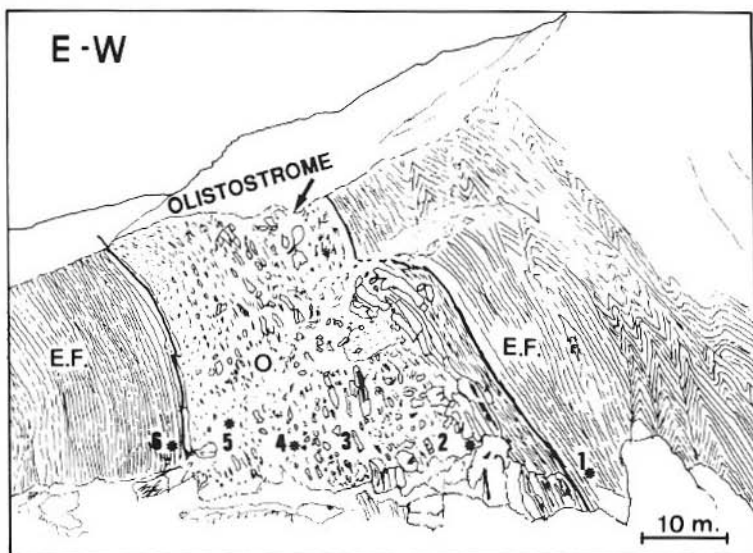


Fig.1.8.- A general view of the inverted olistostrome (O), which is overlaid and underlaid by thin bedded siliciclastic turbidites (sandy flysch, folded and partially inverted) belonging to the Eibar Fm. (E.F.). Numbers 1 to 6 are samples collected for dating purposes.

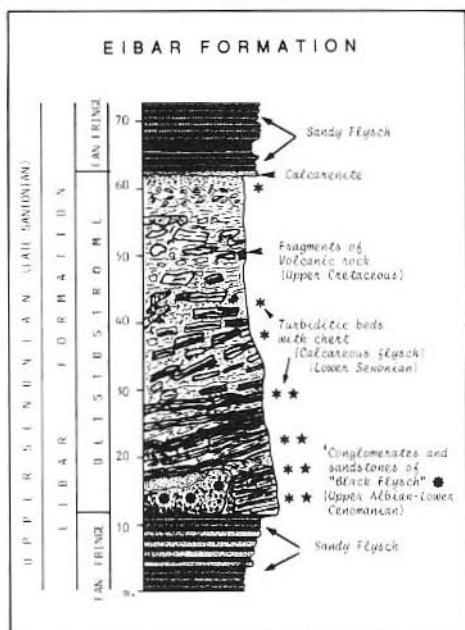


Fig.1.9.- Lithostratigraphic sketch of the Eibar Formation, with the olistostrome under study and with the different types of rocks included in it.

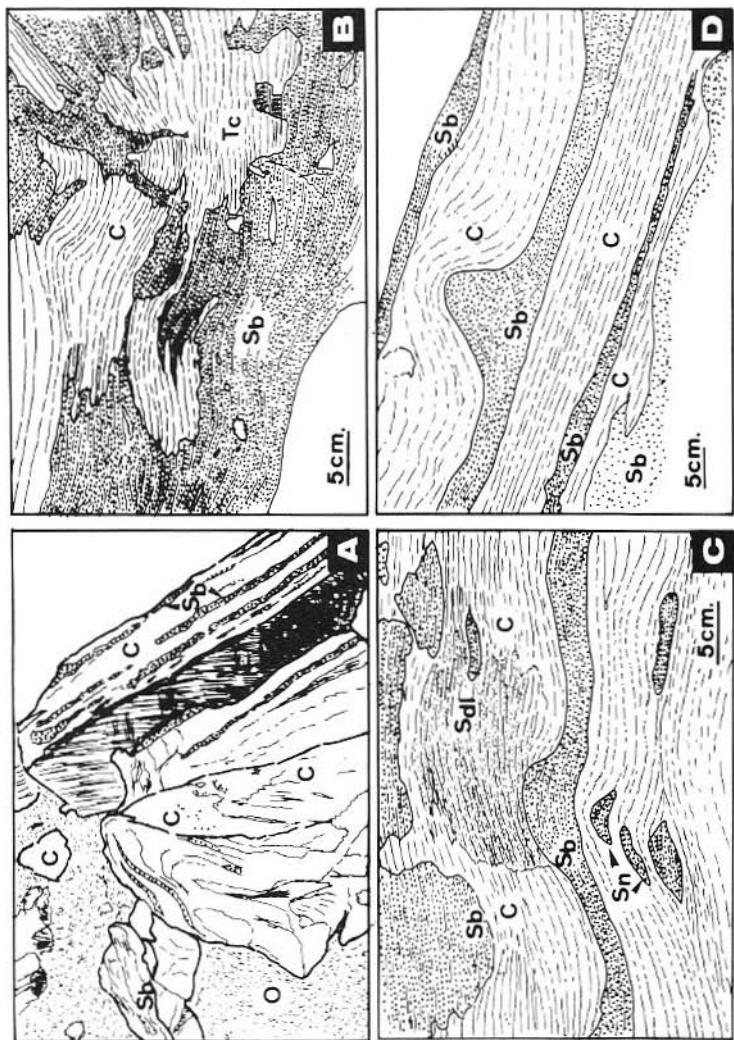


Fig.1.10 A.- A detail of carbonate turbidite blocks (C) with bedded chert (Sb) included in the mentioned olistostrome (O). B.- A detail of silicification (Sb) in calcarenite (C) with convolute lamination. When the silica wupply was low, silicification was patchy. C.- Bedded (Sb), nodular (Sn) chert and chert in poorly-developed laminites (Sdl) replacing primary sedimentary structures. There was a migration and concentration of silica in the anticlinal cores of undulate laminations. D.- Bedded chert (Sb) replacing and preserving the primary sedimentary structures, convolute and planar lamination.

the carbonate host rock, only apparently, did not undergo these modifications (**fig. 1.11 A**). Some examples show a weak remobilization of the silica around the chert fragments (**fig. 1.11 B**). The bedded chert must have been formed before the complete lithification of the carbonate host sediment. Nevertheless, we can also appreciate a clear fracturation at the bottom of some calcarenite beds, with the infilling of fine mudstone that belongs to the lower Te interval.

(2) Chert in poorly-developed laminites.- In this outcrop there is also chert in poorly developed laminites, with the same morphological and petrographical characteristics mentioned above. The sample consists of thin alternating chert and limestone laminae produced by the selective silicification of the Tb and Td intervals (**fig. 1.11 C**). The formation of chert in laminites was early, but apparently not synchronic with the formation of bedded and nodular chert, because the different fibrous silica textures (quartzine and chalcedonite respectively) indicate the existence of silicification under different diagenetic conditions.

(3) Fracture-related chert.- The formation of fracture-related chert was a late-stage diagenetic process that took place after lithification and fracturing of the carbonate turbidite blocks inside the olistostrome, as a consequence of the last readjustment of the turbidite blocks. These fractures cross the bedded chert, nodular chert, and laminite-hosted chert. Along these irregular fractures, the silica-rich fluids migrated and replaced the carbonate host rock which had been already lithified.

The width of the fracture-related chert increases when the fracture passes from the tabular chert to the carbonate host rock (**figs. 1.11 C, D**). A clear remobilization of the early tabular chert near the fracture is visible. **Fig. 1.12** shows a schematic picture of the different chert types, as mentioned in the text.

There are no textural differences in quartz in bedded-, nodular-, and fracture-related chert. All of them mainly consist of microquartz and chalcedonite. The silica contained in this type of chert came from late-stage calcitization (ferroan dolomite) of siliceous organisms or from partial remobilization of silica in the bedded- and nodular chert. We have detected barite by X-ray diffraction in the fracture-related chert.

Mathey (1987) also noted the presence of authigenic barite in the carbonate host rock in the Plentzia Fm. The presence of barite is consistent with the occurrence of quartzine, which in

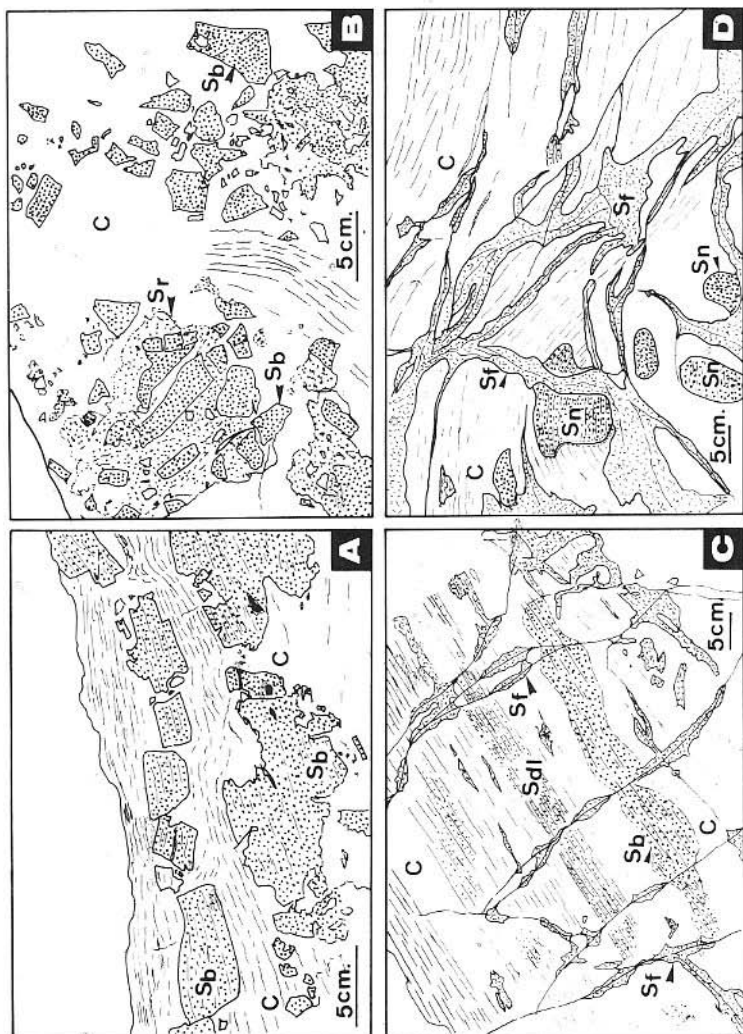


Fig.1.11. A. Fractured and brecciated bedded chert (Sb). The calcarenite (C) here has not been apparently affected B.- Fractured and brecciated bedded chert (Sb) with a small remobilization and recrystallization of the chert (Sr). C and D. - Fractures cross-cutting bedded (Sb), nodular (Sn) and laminite chert (Sdl). These fractures were silicified at a later stage. Note the thickening of fracture-related chert as it crosses the carbonate host rock (C).

pelagic sediments appears always in association with authigenic barite and in many places with dolomite (Keene, 1983).

C) OXYGEN AND CARBON ISOTOPIC DATA OF THE PLENTZIA AND EIBAR FMS.

We have determined the $\delta^{13}\text{C}$ and $\delta^{18}\text{O}$ contents of 22 samples (calcarenites and *Inoceramus* prisms) taken from the Plentzia and Eibar Fms., in the Barrika cliffs (Table IV). These data have been plotted against a lithology section (fig.1.13) to indicate stratigraphic trends.

Oxygen and carbon isotopic values clearly show variations and defined trends through the sequence. In general, the «excursions» or spikes agree with the already known compositional differences in the bulk sediment.

The variations of $\delta^{18}\text{O}$ values obtained from the bulk sediment (calcarenites) are probably related to its burial diagenetic influence, in relation with the presence of more or less ferroan calcite cement.

The oxygen isotopic values of *Inoceramus* prisms can be used for estimating paleotemperatures. If they show no diagenetic recrystallization, then, their oxygen isotopic values are considered to represent the original environmental signal of the bottom water (Schönfeld et al. 1991). But, if the oxygen isotopic composition of *Inoceramus* prisms has more negative values than the relative bulk sediment, recrystallization of skeletal carbonate under conditions of burial diagenesis is suggested.

The $\delta^{18}\text{O}$ values obtained from the *Inoceramus* prisms in the Plentzia Fm. are generally heavier (with a mean of $\delta^{18}\text{O} = -3.64\text{‰}$) than the bulk sediment (calcarenite) with a mean of $\delta^{18}\text{O} = -4.88\text{‰}$. For this reason, the *Inoceramus* prisms can be considered by the moment as unaffected by diagenesis.

The paleotemperatures of the lower-middle Coniacian bottom water, which have been calculated by using *Inoceramus* isotopic values and the equation of Yapp (1979) for the Plentzia Fm., range from 25.6° to 33.7°C with a mean value of 28.4°C. These temperatures have been affected by an early diagenetic modification, and are higher than the values of 12-19°C (with a mean temperature of 16°C) obtained

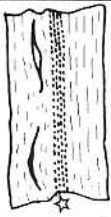
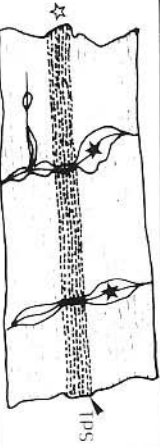


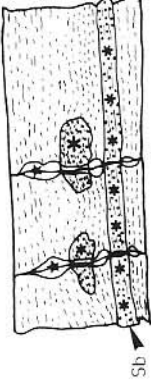


TYPE OF DIAGENETIC SILICIFICATION	PRE-LITHIFICATION OF THE CARBONATE Host-sediment (Turbidite)		COMPLETE LITHIFICATION	POST-LITHIFICATION OF THE CARBONATE Host-rock (Turbidite)
	EARLY SILICIFICATION	FRACTURING AND BRECCIATION OF BEDDED CHERT		
CHERT IN LAMINILS (Sd) ☆		UNAFFECTED	CALCARENITES - CALCISILTITES (Biopel-sparites - biopel-microsparites) CALCAREOUS MUDSTONE	
BEDDED AND NODULAR CHERT (Sb) *				
LATE FRACTURE-RELATED CHERT (SF) ☆				 

Fig.1.12.- Schematic diagram of the different types of diagenetic silicification generated during pre- and post-lithification of the carbonate turbidite.

TABLE IV.- Carbon and oxygen isotopic values of the Plentzia and Eibar Fms.

SAMPLES	$\delta^{13}\text{C}\text{‰(PDB)}$	$\delta^{18}\text{O}\text{‰(PDB)}$
B-26 Sandy flysch (E.F.)	2.09	-4.81
B-25 Sandy flysch (E.F.)	2.34	-4.22
B-22 Calcarenite (Olistost.) (P.F.)	2.27	-3.90
B-19 Calcarenite (Olistost.) (P.P.)	2.18	-3.91
B-24 Sandy flysch (E.F.)	1.75	-4.75
B-23 Sandy flysch (E.F.)	1.87	-5.37
B-35 <i>Inoceramus</i> prisms (P.F.)	1.58	-4.02
B-34 Calcarenite (P.F.)	2.11	-5.03
B-33 Calcarenite (P.F.)	2.43	-4.40
B-32 <i>Inoceramus</i> prisms (P.F.)	1.46	-4.70
B-31 <i>Inoceramus</i> prisms (P.F.)	2.46	-3.25
B-29 <i>Inoceramus</i> prisms (P.F.)	2.23	-3.17
B-28 <i>Inoceramus</i> prisms (P.F.)	2.07	-3.06
B-27 Calcarenite (P.F.)	2.19	-5.23
B-15 Calcarenite with chert (P.F.)	1.83	-4.72
B-11 Calcarenite with chert (P.F.)	1.30	-5.60
B-10 Calcarenite with chert (P.F.)	1.29	-4.90
B-8 Calcarenite with chert (P.F.)	1.79	-4.79
B-5 Calcarenite with chert (P.F.)	2.26	-3.96
B-1 Calcarenite with chert (P.F.)	2.23	-3.30
B-18 Calcarenite without chert (P.F.)	1.24	-5.81
B-1 Calcarenite without chert (P.F.)	0.76	-5.18

(E.F.) - Eibar Fm.

(P.F.) - Plentzia Fm.

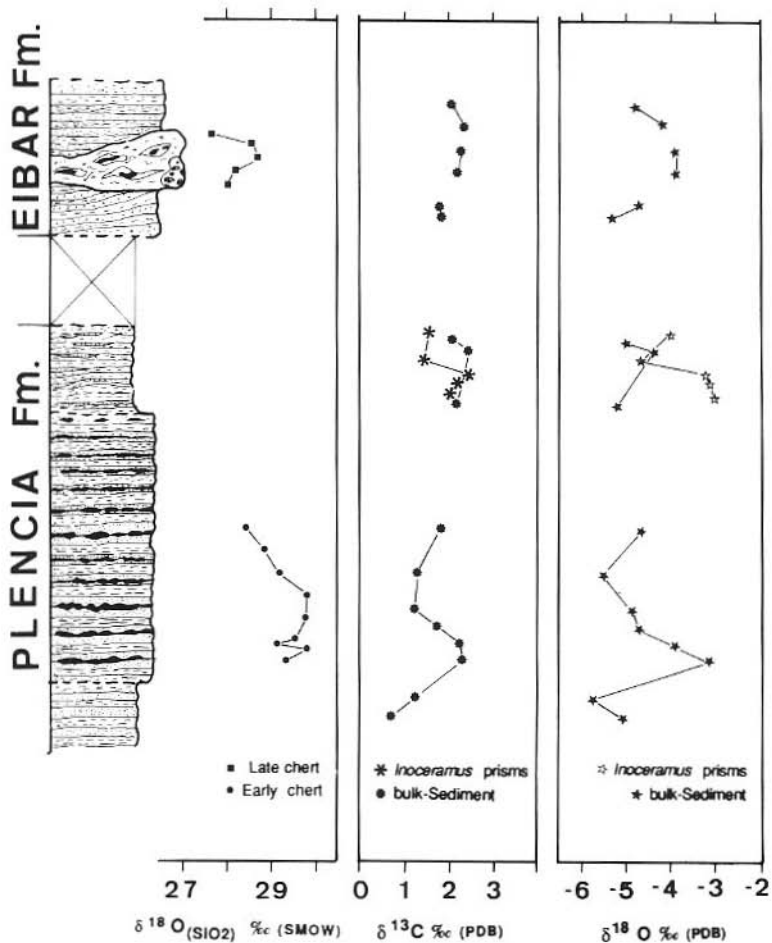


Fig.1.13.- Oxygen stable-isotopic distribution of the cherts (early and late chert). Carbon and oxygen stable-isotopic distribution of carbonate turbidites, *Inoceramus* prisms, siliciclastic turbidites (sandy flysch) and lithostratigraphy in the Plentzia and the Eibar Fms.

by **Schönfeld et al. (1991)** for the Upper Cretaceous Chalk (upper Campanian-lower Maastrichtian) at the Lagerdorf section (NW Germany).

In relation with carbon isotope fluctuations in pelagic carbonates, we assume that the $\delta^{13}\text{C}$ values are unaffected by diagenetic temperature and that they are indicative of paleodepth. At a great scale, the negative accidents are produced in regressive phases, whereas the positive evolution corresponds to transgressive phases, and the anoxic events (OAE) reinforce the transgressive effects (see **Renard, 1987**). If this is correct, the evolutive curve of $\delta^{13}\text{C}$ values will be parallel to the sea-level fluctuation curves of **Hancock and Kauffman (1979)** and **Vail et al. (1977)**.

In our case, we can appreciate important «spikes» (**fig.1.13**) which coincide with the lithologic variations and defined trends along the sequence. In the Plentzia Fm., there exists an important positive spike ranging from 1.24 ‰ to 2.33 ‰ $\delta^{13}\text{C}$ between the calcarenites without chert and the calcarenites with chert respectively, and followed by a fluctuating trend towards the top of the Plentzia Fm. We interpreted this trend as a transgressive event (opening Plentzia trough, **Mathey, 1987**). The mean values from the bottom to the top are 1 ‰ $\delta^{13}\text{C}$ (calcarenites without chert), 1.8 ‰ $\delta^{13}\text{C}$ (calcarenites with chert) and 2.24‰ $\delta^{13}\text{C}$ (calcarenites associated with *Inoceramus*). All these data suggest a clear deepening of the Plentzia basin.

The samples from the Eibar Fm. analysed here have been collected near the inverted olistostrome and show a clear increase towards the top. ($\delta^{13}\text{C} = 1.81$ to 2.21 ‰) which also suggests a deepening in the Orio Trough.



DAY 2. LATE TURONIAN-LOWER CONIACIAN CARBONATE PLATFORMS IN NORTHERN BURGOS

After the generalized Cenomanian-Turonian anoxic event (OAE 3) marked the deepest episode in the nord-Castilian domain, an important sea-level relative fall occurred with the subsequent creation of shallow carbonate platforms in which features indicating sedimentary ruptures are present. This situation most likely corresponds to the limit of 90 m.y. by **Wilgus et al. (1988)**.

Nevertheless, other factors possibly related to the local tectonic activity have been responsible for sedimentary gaps. In fact, several details suggest a close relationship between the platform progradational geometries and the synsedimentary diapiric movements.

As a result of this process, erosional surfaces, paleokarstification phenomena and relic evaporitic textures are not uncommon in the series under study. During the day, we will examine three sections from W to E: Cueva, Bedón Section and El Ribero, respectively (**fig.2.1**). In all of them, several sequence boundaries can be observed, suggesting conspicuous sea-level changes. The diagenetic processes associated with these sea-level fluctuations, as we will see, are very complex and of a varied nature.

THE HORNILLALATORRE, CUEVA AND NIDAGUILA FMS.

The upper Turonian-lower Coniacian sedimentary successions in the Castilian platform domain are represented from the bottom to the top by the Hornillalatorre, Cueva and Nidáguila Fms. (**fig.2.2**) (**Floquet et al., 1982; Floquet, 1991**). The Hornillalatorre Fm. (100-150 m., middle to upper Turonian) is composed by grey marls, nodular limestones and nodular shaly limestones. Its fossil content is relatively poor: echinoids, bivalves (inoceramids and pectinoids), ammonoids and planktonic foraminifera. The unit represents an open platform, which can be external or distal, from circalittoral to infralittoral. The transition to the upper Cueva limestones is relatively gradual but brief, and is represented by some shallowing-upwards sequences.

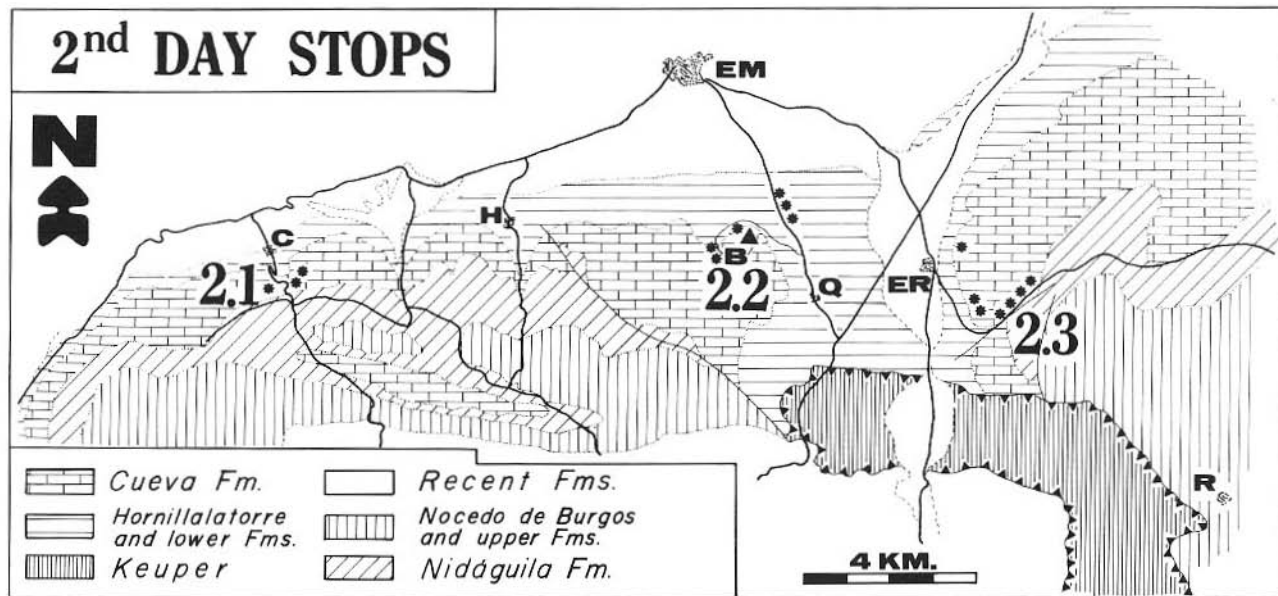


Fig.2.1.- Geographic and geologic location of the threes on the second day. 2.1: Cueva s; 2.2.: Bedón section; 2.3: El Ribero section. C: Cueva; H: Hornillalatorre; B: Bedón peak; E: Espinosa de los Monteros; Q: Quintanaedo; ER: ElRibero; R: Rosío (*marks the itineraries flowed). (Modified from IGME. 1978).

AGE	EBRO NORTH	MENA VALLEY	VITORIA
SANTONIAN			
	NOCEDO DE BURGOS FM.		
CONIACIAN	NIDAGUILA FM.	LOSAS FM.	ZADORRA FM.
		RIBERA ALTA FM.	
TURONIAN	CUEVA FM.	VALLE DE MENA FM.	
	HORNILLALATORRE FM.		

Fig.2.2.- Chart of correlation between the visited Formations (in the northern Ebro and Mena Valley areas) and other equivalent formations in the surrounding areas (Vitoria domain).

The Cueva Fm. (50-80 m., late Turonian-early Coniacian) consists of well-bedded, fine to medium-grained calcarenite (packstone to grainstone), which is massively -stratified at the lower part (in one bank up to 30 m.) and more discrete (a few meters) towards the top. Frequently, the character of its upper half is mixed between marls and limestones. Fossils are not abundant, but representative: corals, sponges, pectinoids, inoceramids, oysters (*Pycnodonte*, some of them appear silicified), miliolids, litiolids and some bioturbations (*Thalassinoides*). The latter are particularly frequent at the upper part of the Fm.

Locally, the Cueva Fm. is strongly dolomitized (El Ribero Member), a phenomenon that will be analyzed during the afternoon (Amiot, 1982; Floquet et al., op.cit.). Particularly, in the neighbourhoods of the Rosío diapir (El Ribero sector), the Cueva Fm. carbonates show progradational morphologies (clinoforms), which will be interpreted in the forthcoming pages. The features of the Cueva Fm. mentioned above seem to be conciliable with an external open platform environment, since it includes very characteristic tidal facies (cross-laminated and cross-bedded bioclastic calcarenites). Its contact with the upper Nidáguila Fm. is typically sharp or poorly-gradual. In some points, the nodular chert is frequent but not particularly abundant.

The Nidáguila Fm. (70-120 m., Coniacian to lower Santonian) is largely composed by grey-bluish marls and shaly limestones, which sometimes bear glauconite and contain oysters (*Pycnodonte*), echinoids, bryozoans, ammonoids, gastropods and brachiopods. Its thickness decreases towards the south, but the litho- and biofacies are practically the same along the whole outcrop area of the unit. The Nidáguila Fm. seems to represent again deeper conditions: an external open platform, infralittoral to circalittoral. Only some oysters and inoceramids are partially silicified and the nodular chert has not been detected in this unit.

MORNING:

FIRST STOP (2.1): THE CUEVA SECTION

A) SEQUENTIAL ANALYSIS

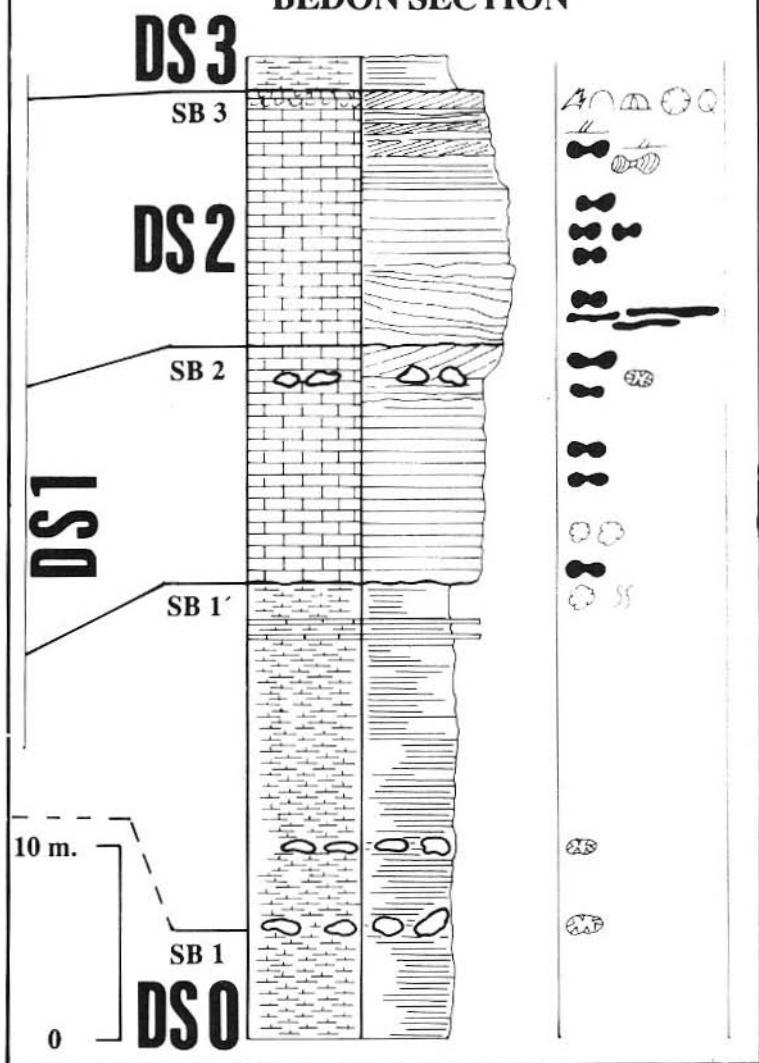
The analysis of carbonate depositional sequences and systems can be made according to very different points of view. However, as a result of the necessity to unify criteria with regard to depositional sequences (vertical facies associations) and depositional systems (lateral facies associations), the philosophy of the so-called «Systems Tracts» has been recently reconsidered (**Van Wagoner et al., 1988**). In this view, a depositional system is a three-dimensional assemblage of lithofacies (**Fisher and McGowan, 1967**) and a systems tract is a linkage of contemporaneous depositional systems (**Brown and Fisher, 1977**). The latter are produced as different environmental associations in accordance with successive sea-level changes regardless of whether they are eustatic or not in origin. For this reason, we can distinguish the Low Systems Tract (LST, indicative of a sea-level fall), the Transgressive Systems Tract (TST, produced during a relevant marine transgression) and the High Systems Tract (HST, indicative of the highest sea-level). A complete interval LST/TST/HST is separated from another by a sequence boundary (SB), can may or may not show erosional features. Some SB's are represented by paleokarst, subaerial exposure surfaces, dessication cracks, etc. The sedimentary and petrographic data allows us to identify three depositional sequences (DS's) limited by sequence boundaries (SB's) which are easily identifiable along the whole visited area.

The lower depositional sequence (DS 0) is represented by the Hornillalatorre Fm. and constitutes an episode indicative of maximum depth (HST 0) during the whole Cretaceous, and associated with an important anoxic event during the Cenomanian-Turonian limit (OAE 3, **Jenkyns, 1980; Renard, 1987**). The top of the HST 0 is the first sequence boundary (SB 1) (**fig.2.3**). It normally marks the limit between the Hornillalatorre and Cueva Fms. However, in the type-area of the Cueva Fm., the (SB 1') sequence boundary mentioned above is located intra-Cueva Fm.. It is irregularly-shaped and characterized by fast limestone/marl transitions. The depressions are filled by marls, tabular sandy limestones and calcarenites which top coarsening-upward sequences at a metrical scale. This fact suggests that the SB 1' in the Cueva section corresponds to a submarine unconformity surface without overt signs of subaerial exposure (**fig.2.4**).

<u>LITHOLOGY</u>	
	Massive limestone
	Limestone
	Bioclastic limestone
	Sandy limestone
	Marly limestone
	Sandy-marly limestone
	Marl
	Sandy marl
<u>SEDIMENTARY STRUCTURES</u>	
	Biostrome/bioherm
	Cross lamination
	Cross bedding
	Erosional surface
	Paleokarstic cavities
	Speleothems and calcite crystals
<u>ADDITIONAL SYMBOLOGY</u>	
	Briozoans
	Echinoderms
	Oysters
	Bivalves (pectinids, inoceramids)
	Gastropods
	Rudists (Hyppuritids)
	Corals
	Bioturbation
	Quartz geodes
	Nodular chert
	Large flattened nodular chert
	Liesegang rings
	Detrital quartz grains
	Pyrite
	Glauconite
	Cross lamination

Fig.2.3.- The Cueva and Bedón stratigraphic sections showing the different depositional sequences (DS) and sequence boundaries (SB). An explanatory legend of the symbols used is provided on the facing page.

BEDON SECTION



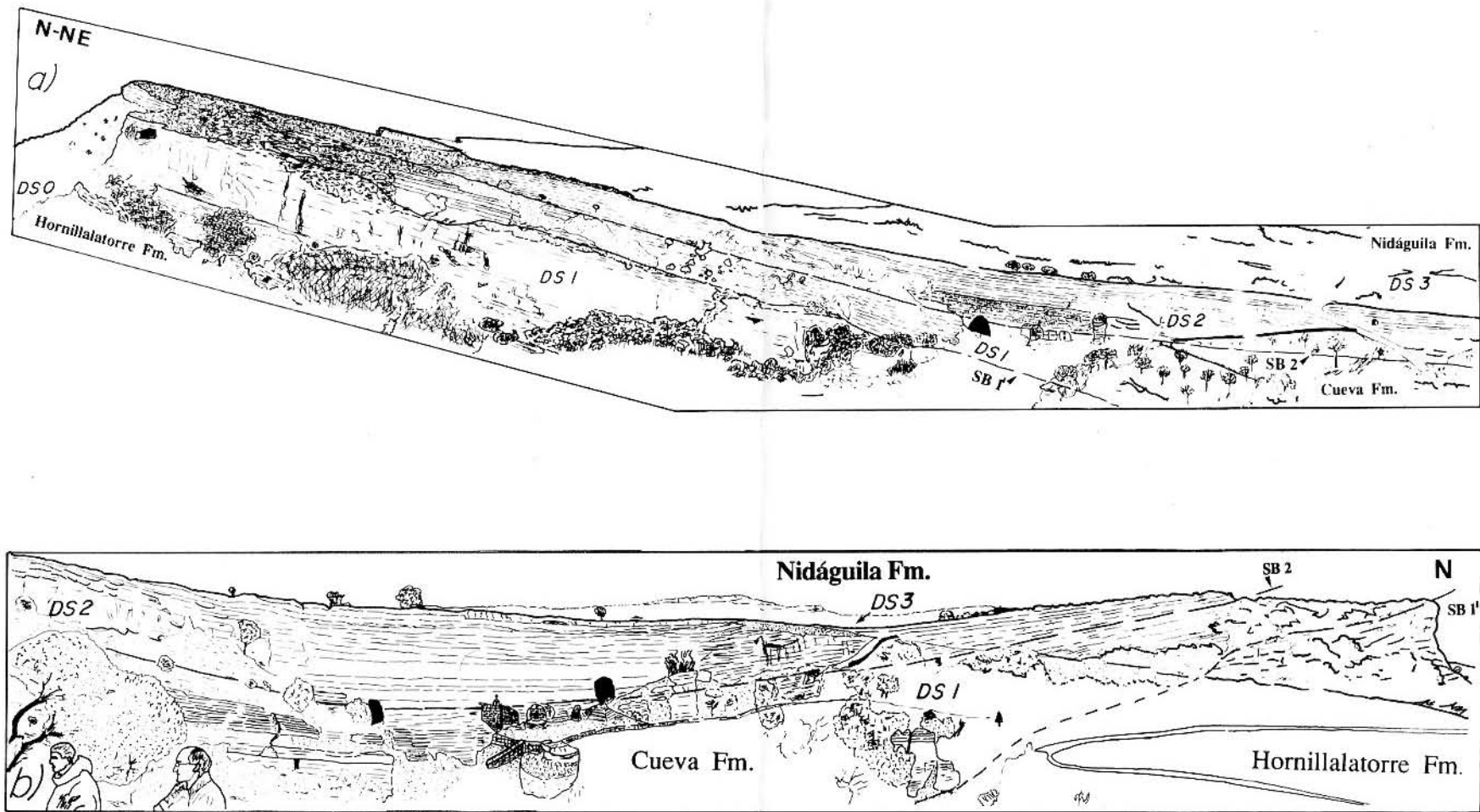
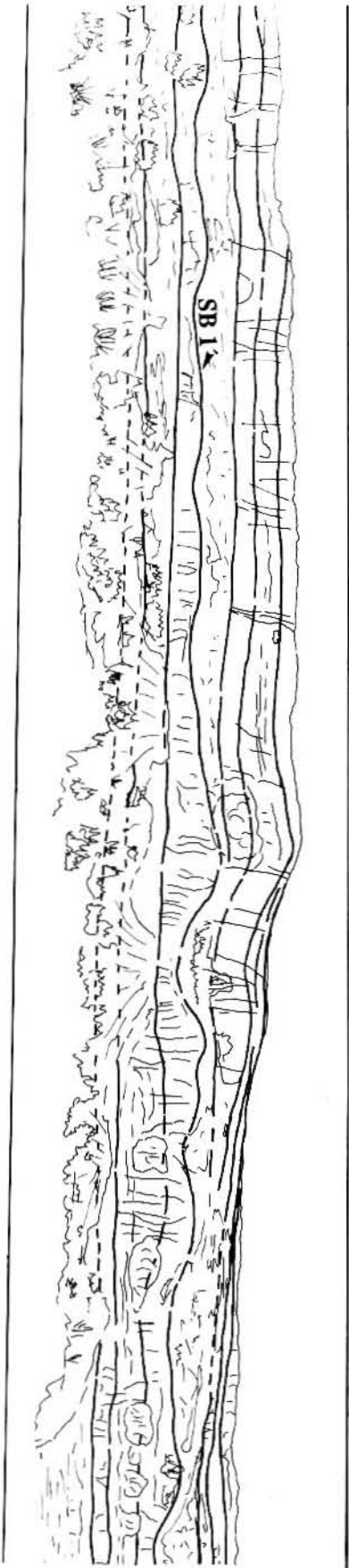
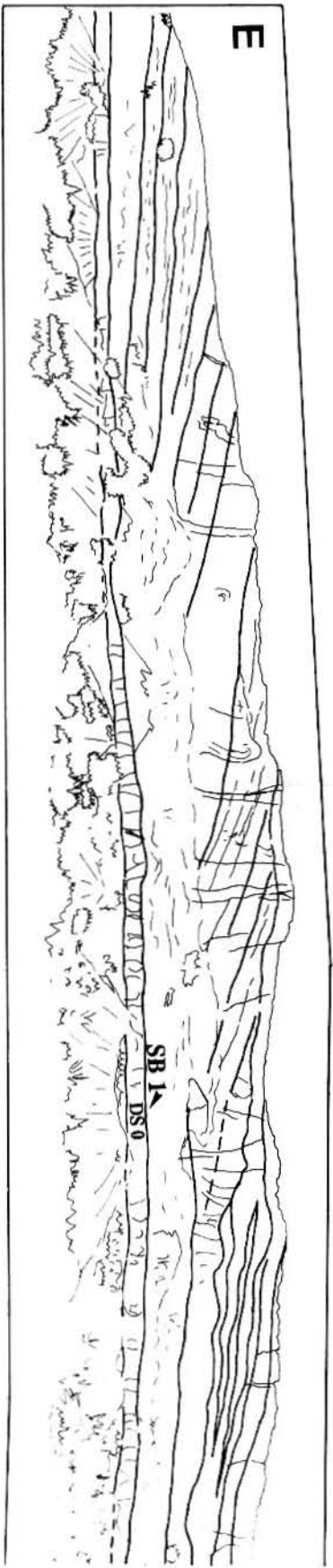


Fig.2.4.- Two panoramic landscapes (a, b) in the Cueva type-section showing the carbonate depositional sequences (DS) and sequence boundaries (SB). The morphology of the carbonate bodies and the erosional features of the SB 1 and SB 2 can be identified.



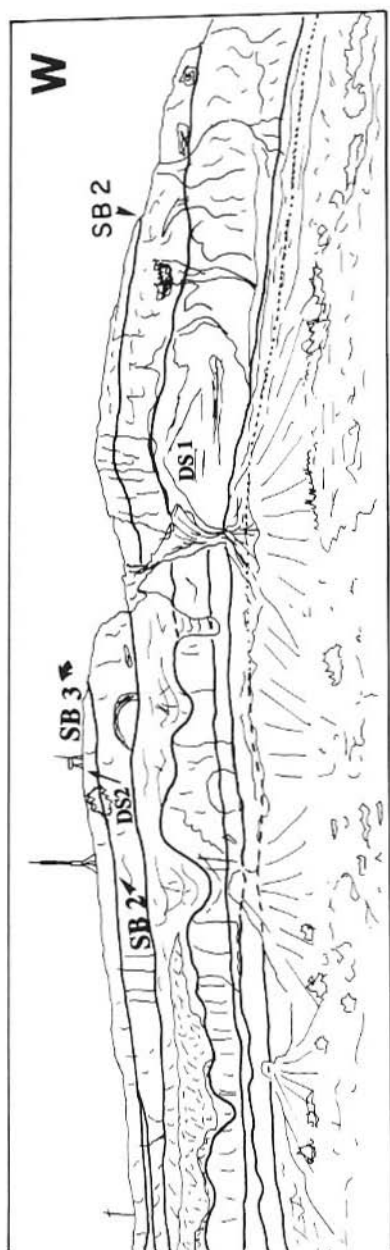


Fig.2.5.- A panoramic landscape corresponding to the Cueva Fm. in the Bedón outcrops. The depositional sequences and the limits between them are observable as well as the progradational morphology (clinoforms), which indicates an outward development of the carbonate platform. (Total outcrop length: 900 m).

The HST 1 (DS 1) is represented by thin-bedded sometimes bioturbated shaly limestone at the bottom. Towards the top, there are calcarenites and biostromic limestones. The calcarenites include oyster, echinoderm and inoceramid fragments. Some marl/shaly- limestone/nodular -limestone shallowing upwards cycles can also be observed. The HST 1 is characterized by framework bioconstruction features: partially-dolomitized coral biostromes (up to 25 cm. thick), which laterally intertongue with bioclastic grainstones. Some hyppuritid shells contain micritic and bioclastic- brecciated infillings which suggests the former occurrence of erosional and destructive processes from storms and/or wave action related to sea-level changes. A cross-bedded limestone body which bears corals and rudists and shows a truncated top seems to have originated from a bioherm flank which has suffered from intense crossive action. This eroded top constitutes the SB 2 sequence boundary, which is onlapped by the DS 2 sediments. It is noteworthy that the SB 2 in all the visited area invariably shows erosional features, that is, truncation surfaces, irregular substrates and sometimes paleokarstic cavities.

The DS 2 sequence has a marked sandy character. Its general trend is organized in shallowing-upward cycles, the shallowest facies appear just near the extreme top of the sequence. In this part of the sequence, there is early nodular chert (nodules up to 25 cm. in diameter) from selectively silicified *Thalassinoides* burrow networks.

Other subvertical and ring-like shaped bioturbations show a glauconitic coating covering their external walls. The glauconitization is particularly observable at the top of the DS 2, specifically, in calcarenites strongly stylolitized in parallelly to stratification planes. The calcarenites also contain oysters, inoceramids, pectinoids and ammonoids. Some geopetal fabrics that affect bivalves can be found as well.

The very top of this sequence is the SB 3, which may be assimilated to that of 88,5 m.y. by **Wilgus et al. (1988)**. Some well-laminated calcite speleothems have been found in association with the SB 3. As we will see, the existence of dolomite in these speleothems leads us to think of ancient karstification processes. The SB 3 precludes a sharp rise of the sea-level which characterizes the DS 3 sequence (Nidáguila Fm., **Floquet et al., op.cit.; Floquet, 1991**).

B) SILICIFICATION

The petrographic evidence is intimately related to the paleogeographic and paleoecological contexts. The silicification processes are conspicuous in the shallowest areas, and appear associated with bioclastic calcarenite beds (grainstones) at the top of the DS 2 (fig. 2.3). The chert appears in several ways: 1) **big nodular chert**, as much as 25 cm. in diameter, some of it controlled by pre-existing *Thalassinoides* burrow systems; 2) partial or total **selective replacement of *Pycnodonte* shells**.

The thin section analysis of the nodular chert chiefly reveals the presence of micro- and cryptocrystalline quartz along with fibrous varieties (chalcedonite) which infill small cavities. The silicification is an early and selective replacement, which preserves the organisms included in the sediment (foraminifers, sponge spicules, etc.) without a previous strong compaction. A biogenic source of the silica (Opal A) seems to be the most plausible one, if we consider the abundance of different types of siliceous sponge spicules preserved within the nodular chert. Evidence of Opal CT precursors, such as quartz-replaced Opal CT lepispheres and rim cements can be found (Maliva and Siever, 1988 b).

It is possible to appreciate that individual euhedral limpid crystals of dolomite appear inside the microquartz mass. Sometimes they have been completely replaced by microquartz, but always show a limpid rhomboidal section.

Numerous *Pycnodonte* and some *Inoceramus* bioclasts are selectively affected by silicification at the top of the Cueva Fm.. Also, these bioclasts are included in the limestone beds of the Nidáguila Fm. In the thin section analysis, the following fabric types can be identified:

- a) Individual spherulites of quartzine-lutecite, replacing foliated microstructure.
- b) Concentric rings of quartzine-lutecite, known as beekite (defined by Hughs, 1889). These rings appear as a series of ridges around a central papilla.
- c) Fine textural replacement by megaquartz in peripheral zones of silicification. The replacement is partial; there is no complete dissolution followed by a filling, since we can see:

- laminar inclusions inside quartzine-lutecite spherulites, with continuance outside.

- the morphologies and orientations of quartz crystals suggest the absence of open cavities in their development.

- the existence of quartzine-lutecite is characteristic of replacement in skeletal fossil fragments.

SECOND STOP (2.2): THE BEDON SECTION

A) SEQUENTIAL ANALYSIS

One of the most outstanding differences between the Cueva Fm. carbonates at the Bedón section and those of the type-section is the existence of progradational morphologies appearing as clinofolds gently dipping an angle of about 4-5° towards the W (**fig.2.5**). This style of presentation is somewhat similar to the one in the El Ribero carbonate platform that we will see in the afternoon, just at the opposite side of the present outcrop area of the Rosío diapir. Thus, the clinofolds observed at local scale suggest that the penecontemporaneous movements of the Rosío diapir closely influenced the carbonate depositional models (**Meiburg et al., 1984**).

The DS 0 sequence is well outcropped along the road from Quintanaedo to the T.V. station just at the head of the Bedón Mountain (**fig.2.1**). The DS 0 sequence is composed by marls and nodular marly limestones, and it becomes more calcarenitic towards the top (**fig.2.3**). The SB 1 is a very flat horizon which bears scarce small quartz geodes and some paleokarstic cavities in association with speleothems.

The HST 1 (DS 1) is composed by a cross-bedded series at the top, coarse-grained calcarenites which include well-developed nodular chert, as well as scarce small quartz geodes. Similarly to the Cueva section, the SB 2 is a truncation surface, but occurs in association with paleokarstic cavities. As we will mention later on, the carbon and oxygen isotopic composition of the speleothem calcite indicate the former presence of a fresh-water environment. In the southern part of the Bedón Mountain and close to the Rosío diapir, an intensive dolomitization which affects a great part of the DS 1 shows features that indicate schizohaline environments (**Folk and Siedlecka, 1974**) which are very similar to those recognized in the El Ribero Member. The SB 1 surface

may be intermediate between the D 2 and D 3 crisis by **Floquet et al. (1987)** and probably coincides with the limit of 90 m.y. estimated by **Wilgus et al. (op.cit.)**.

The entirely calcarenitic DS 2 sequence is composed by cross-bedded series at the base, cross-laminated beds at the top, tabular grainstones which are the host rock for enlarged, conspicuously flattened, silica nodules, some of which show Liesegang rings. At the very top, the cross-laminated calcarenite contains very coarse detrital quartz grains suggesting a beach environment (foreshore). The top of the last calcarenite bed marks the SB 3 sequence boundary.

B) SILICIFICATION.

The silicification in the Bedón section sediments appears in several ways:

- 1) **big chert nodules**, some of which are controlled by pre-existing *Thalassinoides* burrow systems.
- 2) selective anhydrite nodule replacements developing **quartz geodes**.
- 3) **selective replacement of oysters (*Pycnodonte*) and *Inoceramids***.

The nodular chert in the Bedón section appears immediately over the SB 1' and follows along the DS 1 and DS 2 sequences. Unlike this early manifestation, in the Cueva section, the first occurrence of nodular chert is over the SB 2. This difference in time suggests a greater diapiric influence in the former area.

The appearance and development of the nodular chert reasonably coincides in time with the so-called «belt of maximum flint» near the top of the Turonian in the English Chalk and that of Northern France and Northern Germany (**Mortimore and Wood, 1986**). The brief time of deposition of the sediments that constitute the Cueva Fm. and the limited number of nodular chert horizons are not in disagreement with the possibility pointed out by **Ehrmann (1990)** about the relationship between the rhythmic occurrences of flint layers and the variations in the earth's orbital parameters (Milankovitch cycles).

The thin section analysis of the nodular chert and selective oysters replacement reveals very similar fabrics at the Cueva section described below.

The formation of small quartz geodes (cauliflower-like) is a characteristic diagenetic process in the Cueva Fm. sediments. The small quartz geodes can be abundantly found below the SB 1' and exceptionally detected a few meters above the SB 1' at the Bedón section.

The quartz geodes are spherically- to subspherically- shaped, and correspond to the «cauliflower» type of **Chowns and Elkins (1974)**. Their diameter varies from 1 to several cm. and inside, we can observe compact masses of carbonate filling the inner void as a later process.

The silicification process is represented on the geodes by several rather concentric bands, which can be briefly described from the outside to the inside as follows:

1) A **megaquartz** band with heterometric crystals (puzzle-like shape), with undulose extinction and sutured boundaries, becomes rectilinear. This band which acquires a quasi- polygonal texture is very uncommon to find.

2) A band of **quartzine and lutecite spherulites**, much more developed than the previous one, and with a clear intergrowth of the spherulites, until they reach the inner band. The spherulites reach a size of 1-2mm. with more or less irregular shapes. Sometimes, the nuclei present a clear linear disposition.

3) A **megaquartz** band which can be generated directly from the second band as a consequence of the continuous growth of the quartzine and lutecite fibres; usually this growth is gradual, showing the process step by step until the texture of the prismatic and long megaquartz ends in perfectly defined faces.

Many petaloid megaquartz crystals with inclusions and cubic sections are found. In the megaquartz crystals, we find many different types of inclusions: a) Small anhydrite inclusions which follow no fixed pattern can be either homogeneously spread in the megaquartz, or leave a fine clean exterior rim in the euhedral sections. b) Inclusions of anhydrite concentrated in the nucleus of the megaquartz with polygonal textures. c) Undetermined opaque-brown color inclusions, which are probably the result of organic residues included in the primitive anhydrite. d) Large individual carbonate (dolomite) crystal inclusions, sometimes

spherically-shaped, and isolated. The carbonate crystals seem to derive from an earlier development and have smaller anhydrite inclusions.

The quartz geodes are considered the result of the replacement and void filling of previous anhydrite nodules by different textural types of quartz, during a complex diagenetic process. In this section, the geodes are associated just below the SB 1' which is a good indicator of the shallowing upward tendency of the DS 1 sequence.



LUNCH: LOS ROBLES RESTAURANT

AFTERNOON:

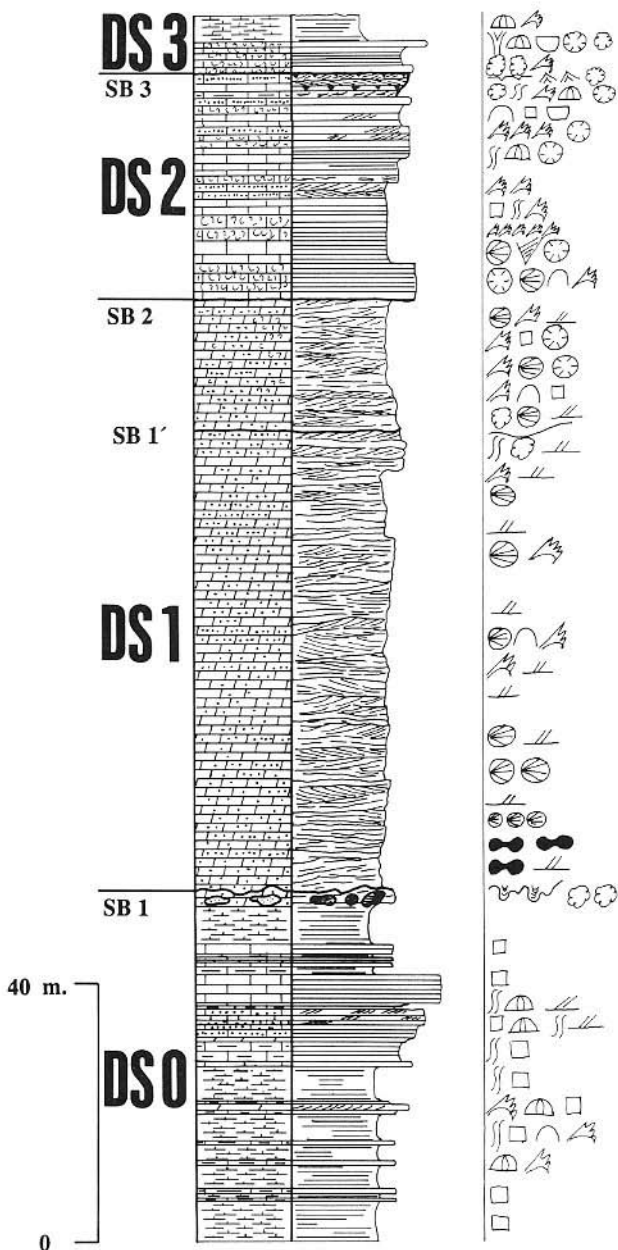
THIRD STOP (2.3): THE EL RIBERO SECTION

The Cueva Fm. is intensely dolomitized in a specific area near the El Ribero town (**fig.2.1**). The diagenetic lateral change of facies from dolomitized to non-dolomitized rock is easily identifiable from the parking of the «Preciado» Restaurant. For this reason, the «Dolomías de El Ribero» (El Ribero Dolomite) has been categorized as a member of the Cueva Fm. by **Floquet et al. (1982)**. These authors have proposed the hypothesis that this member originated from the uplift of the Rosfo

LITHOLOGY	
	Limestone
	Bioclastic limestone
	Sandy limestone
	Marly limestone
	Dolomite
	Sandy dolomite
	Bioclastic dolomite
	Marl
	Sandy marl
SEDIMENTARY STRUCTURES	
	Cross lamination
	Erosional surface
	Paleokarstic cavities
	Well-laminated sediment infilling karstic cavities
	Mud-cracks
ADDITIONAL SYMBOLOGY	
	Sponges
	Briozoans
	Echinoderms
	Oysters
	Other bivalves (pectinids, inoceramids)
	Gastropods
	Corals
	Coral build-ups
	Mud mounds
	Bioturbation
	Radial calcite geodes
	Quartz geodes
	Nodular chert
	Pyrite
	Symmetrical ripples
	Cross lamination
	Mud-cracks

Fig.2.6.- The El Ribero stratigraphic section showing the different depositional sequences (DS) and sequence boundaries (SB). An explanatory legend of the symbols is provided on the facing page.

EL RIBERO SECTION



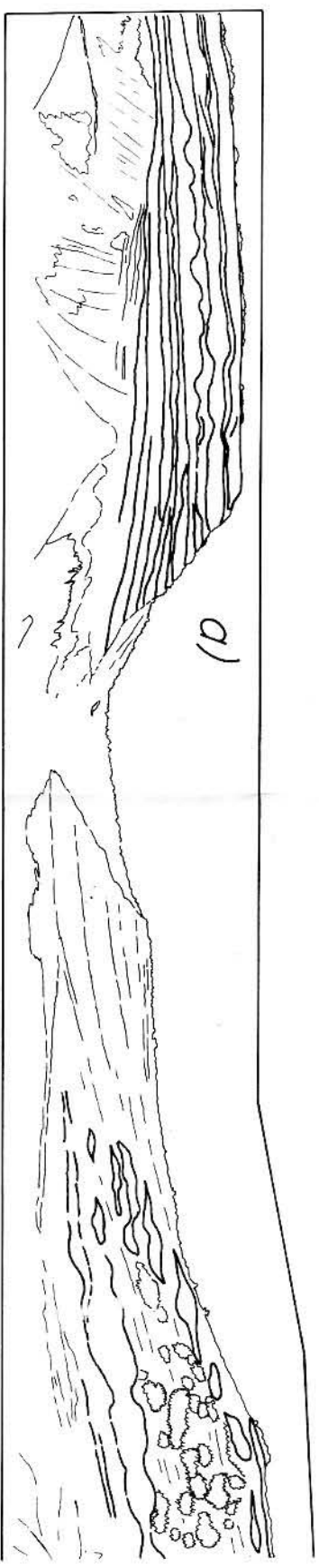
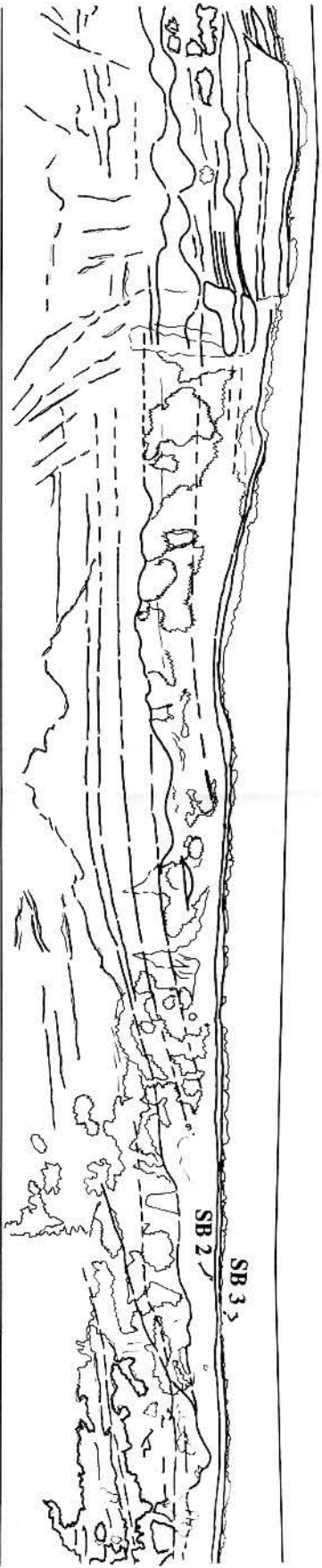
diapir. As will be seen, several sedimentary and diagenetic features do not contradict this idea, but they tell us about a very complex depositional history. In any case, the El Ribero area is crucial for an accurate enlightening of the carbonate depositional models and their evolution during the upper Turonian-lower Coniacian interval.

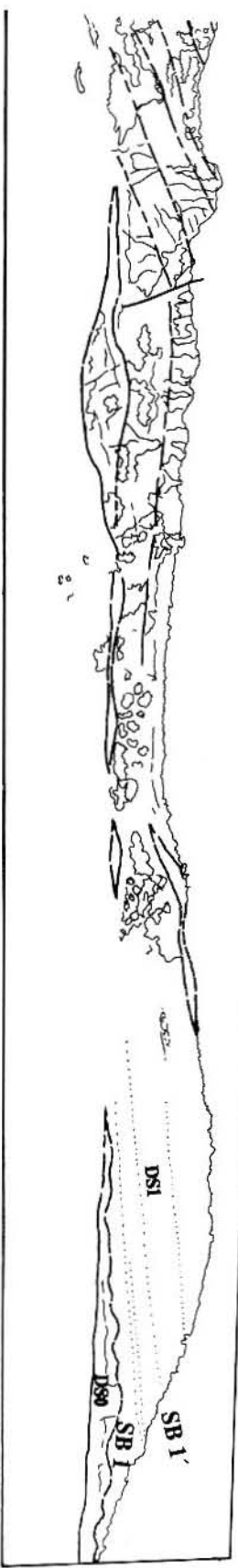
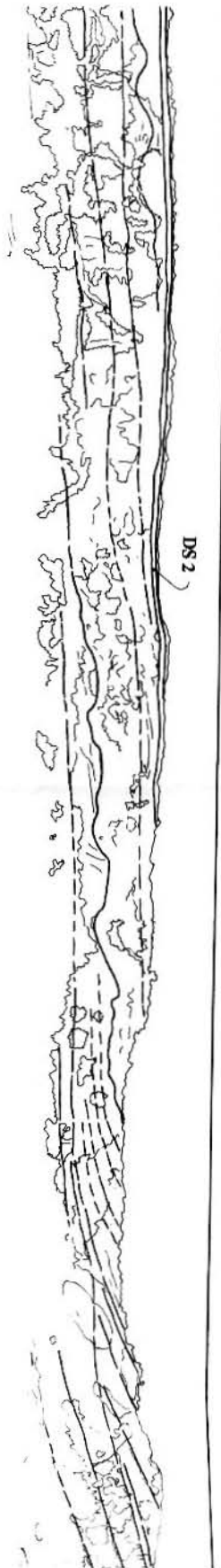
A) SEQUENTIAL ANALYSIS

As in the two former stops, we have established a sequential arrangement according to the Systems Tracts theory proposed by **Van Wagoner et al. (1988)**. The field and microscopic evidence allows us to identify three depositional sequences (DS), which correlate with those of the Cueva and Bedón sections and are limited by three sequence boundaries (SB) (**figs.2.6, 2.7**), some of which show erosional outlines and perhaps not all of which are related to pure eustatic sea-level changes, but local, diapir-originated ones.

The lower depositional sequence (DS 0) (**fig.2.6**) includes, at the bottom, the deepest marly facies of the upper Cretaceous sediments in the Navarro-Cantabrian domain (High Systems Tract, HST 0, Hornillalatorre Fm.). They are topped by metrical-scale shallowing-upwards cycles (**fig.2.8, stage 1**) that contain echinoderms and oysters and show an intense bioturbation. Just at the top of the HST 0 (DS 0), the first sequence boundary (SB 1) is represented by irregular surfaces showing several paleokarstic cavities (**fig. 2.8, stage 2**), which suggests a first episode of relative sea-level fall (Low Systems Tract, LST 1). The isotopic data (C/O) of a well-laminated calcisiltite filling the karstic cavities suggest a deposition in a meteoric water environment. This fact, together with the erosional and slightly angular character of the unconformity, and the formation of small quartz geodes of less than 1 cm. in diameter, indicates a type 1 SB which is clearly correlated with that of 90 m.y. by (**Wilgus et al., 1988**).

The HST 1 (DS 1) is very well developed. It is characterized by an organization in clinofolds or progradational morphologies generally dipping towards the N and NE (**fig.2.8, stages 3 to 6**). On the other hand, opposite and variable inclinations in some places indicate substrate tiltings possibly related to the halokynetic movements of the adjacent Rosío diapiric zone (**García-Garmilla and Elorza, 1989**). Some minor gaps in the clinofold system also can be detected (**fig.2.8, stage 5**). The presence of abundant nodular chert is remarkable in different horizons, particularly in the northernmost clinofolds (El Ribero quarry) (**fig.2.8, stage 6**). Close to the present-day diapiric area, there is an





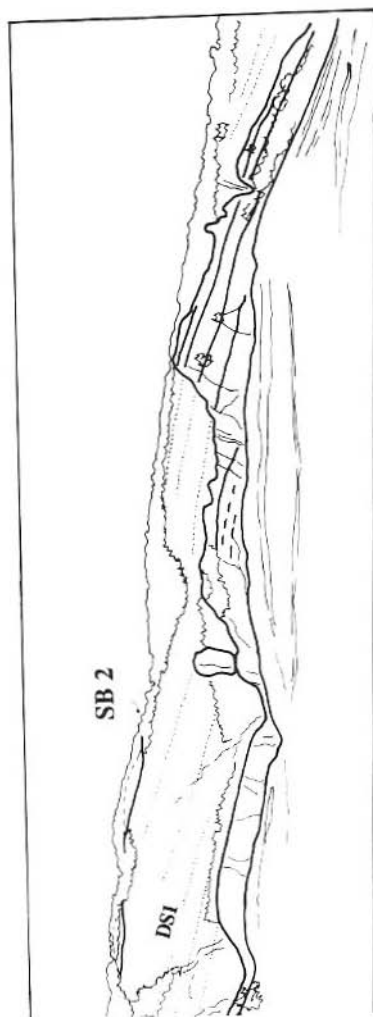
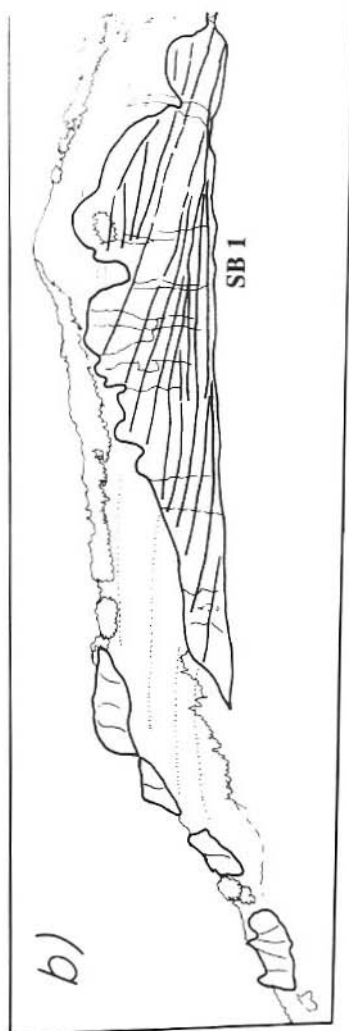


Fig. 2.7.- Two panoramic landscapes of the Cueva Fm. The two outcrops shown are related to the present day exhumation area in the Rosío diapiir. The northern section (a) shows the very spectacular clinoforms which mark a lateral accretion of the carbonate platform towards the N

and NE. The southern section (b) reveals a progradation in the opposite direction with regard to the former. This suggests the influence of the diapiric movements upon the development of the carbonate platforms in this area. (Total outcrop lengths: a) 2200 m. b) 1000 m.)

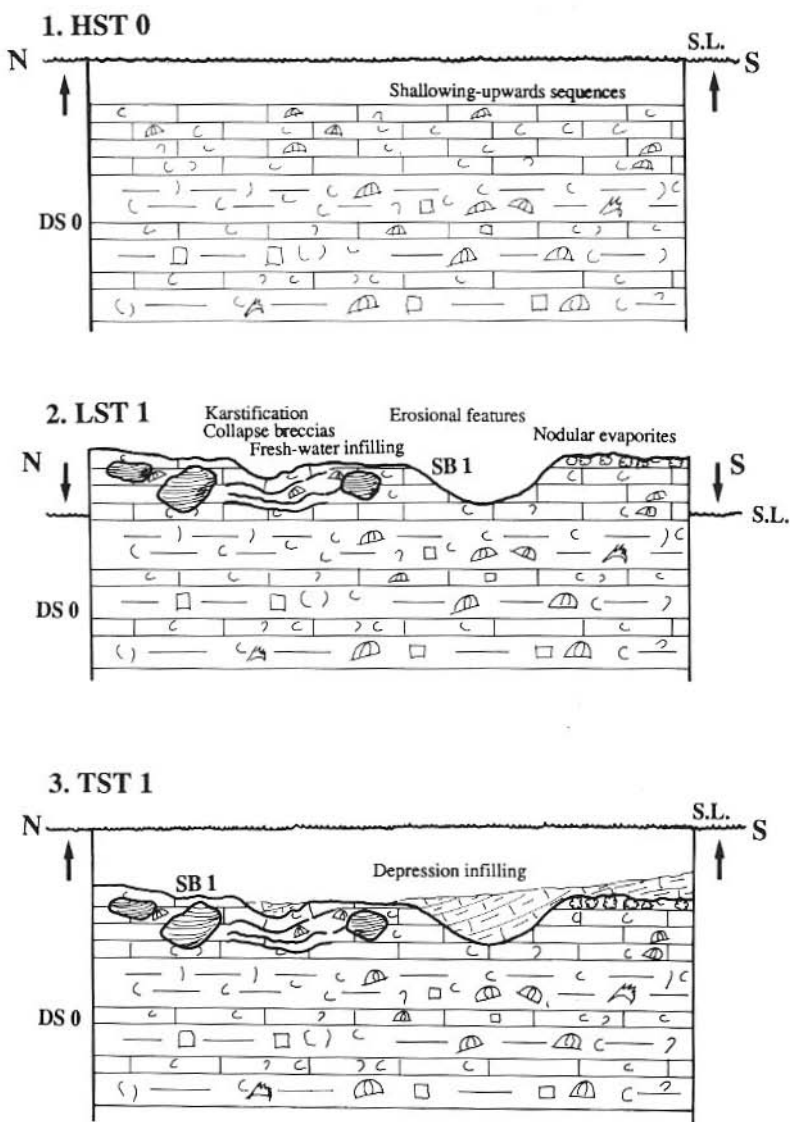
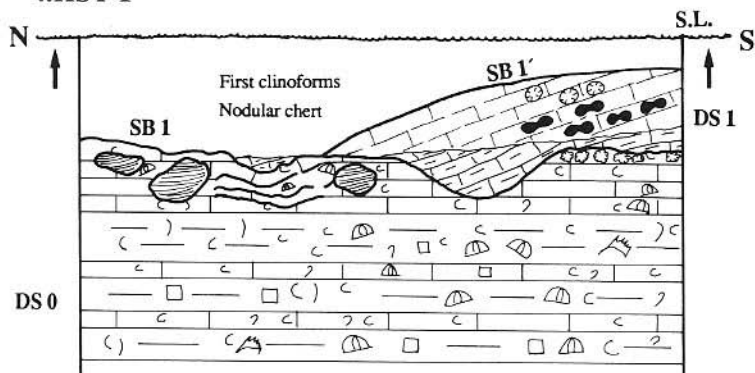
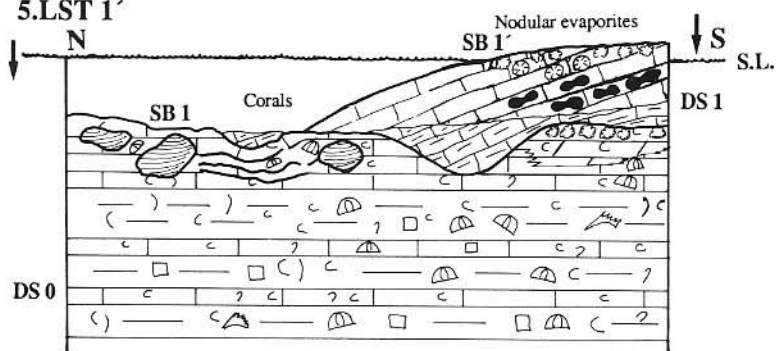


Fig.2.8.- Diagenetic/depositional schemes showing a possible interpretation of the El Ribero carbonate platform history. 1: the HST 0 corresponds to the final time of deposition of the Hornillatorre Fm. (DS0). 2: as a result of the LST 1 episode, erosional surfaces and paleokarstification cavities are produced. 3 and 4: the TST 1 and HST lead to the development of infilling deposits and, subsequently, to the formation of the first clinoforms. The earliest silica nodules were probably formed at this stage. 5: the LST 1 'contains nodular evaporites. 6: the TST 1 - HST 1 is strongly developed. Coral build-ups, the largest chert nodules, radial calcite geodes, dolomitization and the bigger clinoforms are developed at this stage. 7: from LST 2 to LST 3, the very shallow DS 2 sequence includes cauliflower-type geodes at the top. Also, the mud-cracks are filled by silica. This is the top-lap sequence which conspicuously thickens and outwards to the Mena Valley domain. 8: The TST 3 (DS 3) is the base of the Losas Fm. which marks a clear deepening in the sedimentary setting.

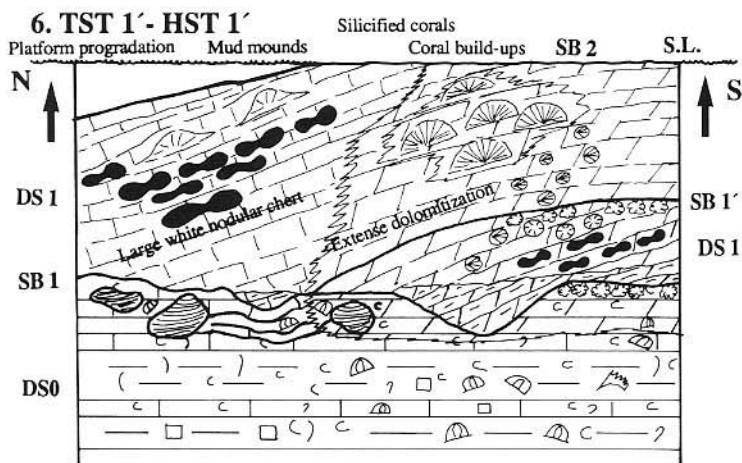
4.HST 1



5.LST 1'

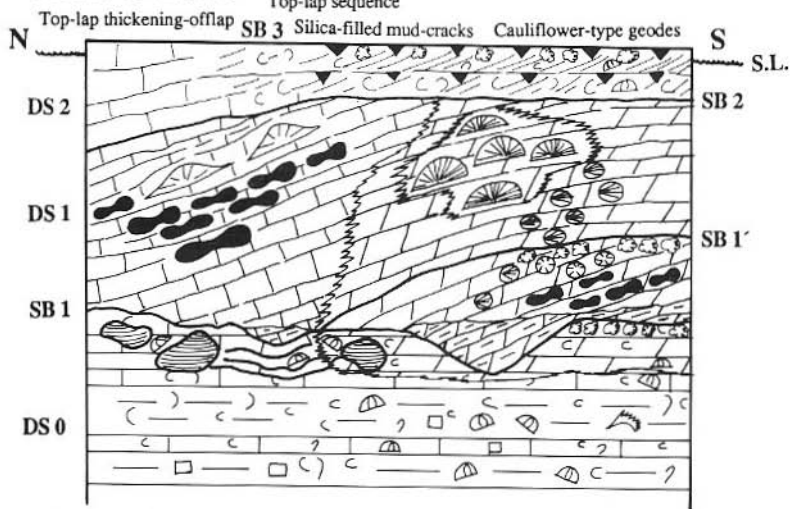


6. TST 1' - HST 1'

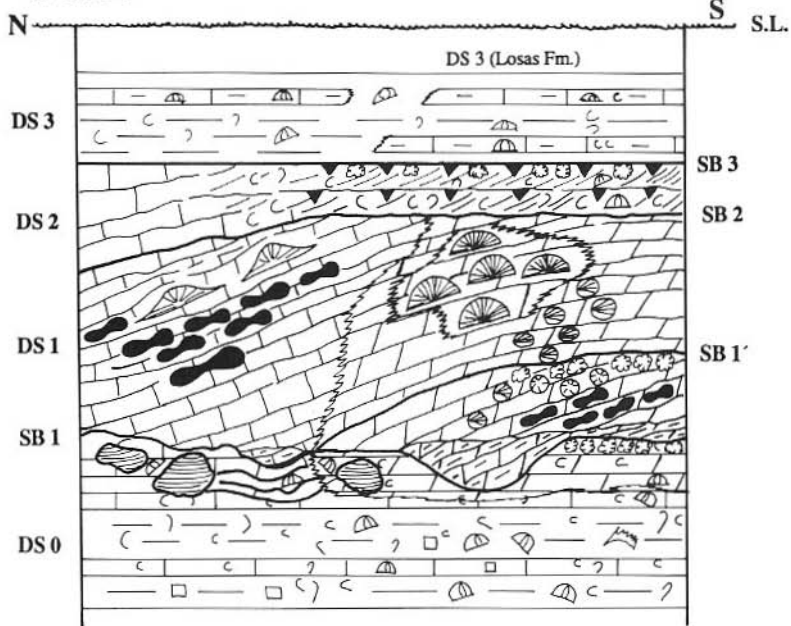


7. LST 2 - LST 3

Top-lap sequence



8. TST 3



intense dolomitization affecting several tens of meters of the sedimentary pile, but the sedimentary structures (cross-lamination and truncation surfaces) denoting a shallow high-energy environment are optimally preserved.

Several diagenetic features point out a general schizohaline environment in the sense of **Folk and Siedleka (1974)**. On the one hand, the hypersalinity conditions are represented by small quartz geodes including megaquartz with relic anhydrite laths, length-slow chalcedony and very fine crystalline dolomite. On the other hand, the euhedral limpid dolomite crystals, the coarse poikilitic sparry calcite (sometimes as nodular shapes with radiaxial fibrous crystals) and the zoned dolomite are considered as having originated under hyposaline regimes. As we will see later on, the carbon and oxygen isotopic composition of radiaxial calcite reinforces the evidence for a fresh-water input. These schizohaline conditions could be in close relationship with the local diapiric movements described by **Meiburg et al. (1984)**.

The DS 2 sequence is represented by a subhorizontal calcarenite top-lap, which lies directly upon the clinoform system of the HST 1 as an angular unconformity surface (SB 2) and represents a relative stillstand of the sea-level (**fig.2.8, stage 7**). The DS 2 evolves to a thickening outward offlap (**Bosellini, 1984**) towards the northern area (Valle de Mena). It is composed by upwards-shallowing cycles ranging from ill-structured limestone beds at the bottom to cross-laminated, bearing plenty of bioclasts — corals, echinoderms, sponges, oysters and other bivalves — calcarenite beds crowning the sequence. At the very top, the shallowing features are conspicuous: small quartz geodes and quartz-filled dessication cracks in different horizons characterizing the SB 3 sequence boundary. This limit may be assimilated to that of 88,5 m.y. claimed by **Wilgus et al. (op.cit.)**.

Finally, the following DS 3 depositional sequence (**fig.2.8, stage 8**) denotes a sharp rise of the sea-level, and its background sedimentation largely consists of marls bearing echinoderms and oysters (Nidáguila and Losas Fms.).

B) SILICIFICATION, DOLOMITIZATION AND CALCITIZATION.

Three main diagenetic processes have been detected: silicification, dolomitization and later calcitization. Possibly, the former is

the earliest one. The nodular chert shows microscopic and megascopic characteristics which suggests an origin prior to the compaction of the host sediment. The source of the silica is clearly biogenic. This claim can be supported by a number of siliceous sponge spicules preserved inside the chert nodules.

The silica can be found under different forms: 1) replacing **corals**, some of them in living position; 2) as **chert nodules**, relatively scarce in the central part of the El Ribero area, but better represented towards the south in the lower series and the north in the upper series of DS 1; 3) **quartz geodes** along the SB 1 and SB 3 surfaces including anhydrite laths. They also appear in the central part of the stratigraphic section (SB 1') in association with silicified corals. There is also silica replacing **mud-cracks** which bears evaporitic precursors in relation to SB3; 4) silicified **oysters** (*Pycnodonte*) and *Inoceramids*. In a few cases, two generations of «beekite» are observable.

The extensive dolomitization is an exclusive process related to the Rosío diapiric area. This leads us to think of a progressive shallowing trend as a result of the continuous halokynetic movement, as claimed above.

The obscure fine crystalline rhombohedra mosaics are the commonest type of dolomite, whose nuclei are frequently surrounded by limpid dolomite rims. This late limpid dolomite can be seen as isolated euhedral crystals surrounded by blocky or poikiloblastic calcite. In other cases, the nuclei are coated by alternating generations of very minute bands of calcite/dolomite.

Finally, the sparry and poikiloblastic calcite together with the coarse-crystalline radiaxial calcite nodules represent the latest diagenetic phase and indicate an important meteoric water input, as will be seen below.

This intense calcitization process fundamentally affects the DS 1 sedimentary pile, which is limited from the SB2 to the SB 1 surfaces in the El Ribero section.

ISOTOPIC DATA

In order to confirm the obtained general petrographic information, we have analyzed the oxygen and carbon isotopic com-

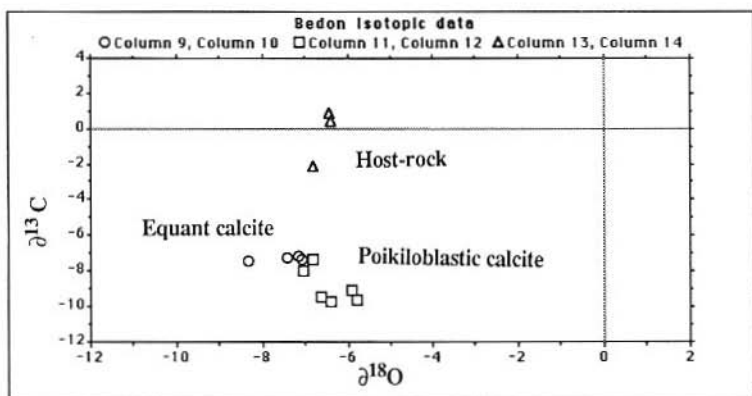


Fig.2.9.- Isotopic data from the Bedón section.

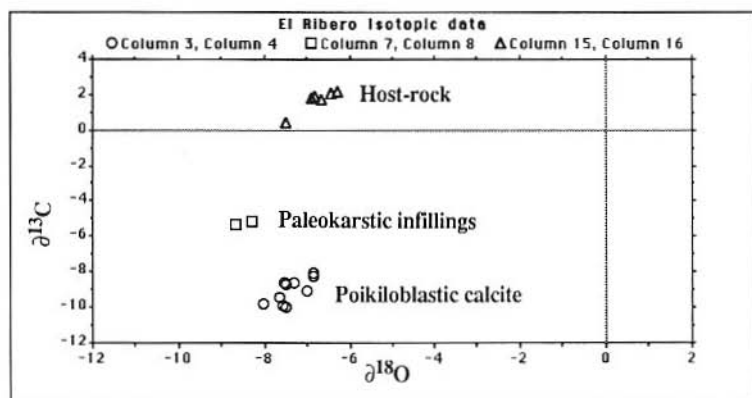


Fig.2.10.- Isotopic data from the El Ribero section.

position of 19 samples of the Bedón section and 18 samples of El Ribero section.

In the Bedón section, we have analysed: the marine limestones (host rock) with a high content in marine fauna (3 samples); the equant calcite (4 samples) in association with syndepositional fractures in the dolomitized area; and 12 samples of poikiloblastic calcite, which constitute the most important evidence of the late strong calcitization undergone by the sedimentary pile.

The values $\delta^{18}\text{O}$ and $\delta^{13}\text{C}$ plotted (**fig.2.9**) are included inside the meteoric cements of Enewetak Atoll area (in **Moore, 1989**) with small $\delta^{18}\text{O}$ variations and large $\delta^{13}\text{C}$ variations characteristic of meteoric diagenesis. This trend follows Lohmann's meteoric calcite line (**Lohmann, 1988**).

The mean isotopic values are as follows:

Host rock ($\delta^{18}\text{O} = -6.56\text{‰}$; $\delta^{13}\text{C} = -0.29\text{‰}$);

Equant calcite ($\delta^{18}\text{O} = -7.49\text{‰}$; $\delta^{13}\text{C} = -7.28\text{‰}$); Poikiloblastic calcite ($\delta^{18}\text{O} = -6.49\text{‰}$; $\delta^{13}\text{C} = -8.79\text{‰}$).

With regard to the El Ribero section, 18 samples have been analysed and the resulting values, $\delta^{18}\text{O}$ and $\delta^{13}\text{C}$, have been plotted, as illustrated in (**fig.2.10**): the marine limestones (host rock) (6 samples); the paleokarstic infillings below the SB1 (2 samples); and the poikiloblastic calcite directly associated with the late calcitization (10 samples).

The mean isotopic values are the following:

Host rock ($\delta^{18}\text{O} = -6.76\text{‰}$; $\delta^{13}\text{C} = +1.69\text{‰}$);

Paleokarstic infillings ($\delta^{18}\text{O} = -8.48\text{‰}$; $\delta^{13}\text{C} = -5.23\text{‰}$);

Poikiloblastic calcite ($\delta^{18}\text{O} = -7.38\text{‰}$; $\delta^{13}\text{C} = -9.05\text{‰}$).

The plotted values are included in the area of the meteoric cements of Enewetak Atoll, with small variations of $\delta^{18}\text{O}\text{‰}$ and with more important variations of $\delta^{13}\text{C}\text{‰}$, which are characteristic of a meteoric diagenesis that affects the marine sedimentary pile.

It seems obvious that there exists a genetic relationship among the poikiloblastic and equant calcite of the Bedón section and the poikiloblastic calcite of the El Ribero section, all of which were

originated during the latest calcitization process associated with a dominant meteoric water input.



*El Ribero. The Alvarado-Velasco House
(XVth c.)*

DAY 3: THE PLATFORM MARGIN AND THE TRANSITION TO BASINAL ENVIRONMENTS

THE VALLE DE MENA, RIBERA ALTA AND LOSAS FMS.

There are certain faciological differences between the upper Turonian-lower Coniacian carbonates in the North-Castilian platform and those more or less equivalent in age in the Navarro-Cantabrian Trough (**fig.0.1**). A scheme of correlation between the Turonian-Santonian Fms. in the region can be seen in **fig.2.2**. Basically, the Fms. in the Navarro-Cantabrian Trough seem to have been deposited in environments deeper than their equivalents in the Northern-Castilian platform, nevertheless, the local influences of tectonism and diapirism could possibly have played an important role in the mechanisms of sedimentation and/or biogenic production of carbonate. In fact, the fossil content in the sediments is not particularly abundant, but notably increases in the relative paleotopographic «highs», in which sponge and coral build-ups and framestones are well-represented. For this reason, it is difficult to identify the exact point of transition between the two

tecto-sedimentary domains. Be that as it may, the excursion this morning deals with distal platform environments and their intertonguing with basinal ones.

The upper Turonian-lower Coniacian sedimentary successions in the Navarro-Cantabrian domain are represented from the base to the top by the Valle de Mena, Ribera Alta and Losas Fms. (**Amiot, 1982**). The Valle de Mena Fm. (250-1300 m., Turonian save early) is largely composed by shaly and sandy limestones and marls bearing inoceramids and globotruncanids. Its maximum thickness is in the neighbourhood of the Angulo mountain pass. On the other hand, near the Bercedo village, the Fm. is only 250 m. thick. Probably, these sediments were deposited in a relatively deep strongly-subsiding basin.

The Ribera Alta Fm. (120-150 m., lower Coniacian) is by far the most spectacular of the three Fms. of the Turonian-Coniacian interval in the Navarro-Cantabrian Trough. This Fm. stands out conspicuously between the El Ribero section and the Subijana village. From this point to the E, the Fm. laterally passes to the Zadorra Fm. (**fig. 2.2**). The latter is indicative of a deep basin environment which includes turbidite beds. Thus, in Subijana, we can observe the transition from the distal platform (Ribera Alta Fm.) to the basin (Zadorra Fm.). The Ribera Alta Fm. is composed by bioclastic limestones and calcarenites which alternate with very few and scarce marly episodes. Oysters (*Pycnodonte*), *Inoceramids*, pectinoids, litiolids and miliolids, together with coral and sponge fragments are the most representative fossils in this unit. The morphological, biofaunal and sedimentary data lead us to think of a very widespread distal platform setting for the Ribera Alta Fm. Furthermore, the field observations allow us to conclude that the development of the carbonate platform was the result of the thickening-outwards of the top-lap at the upper part of the El Ribero platform (**García-Garmilla and Elorza, 1989**). As we can see in the Subijana section, the massive aspect of the carbonate banks becomes in mound-shape morphology with fast lateral developments towards associated facies.

Finally, the Losas Fm. (360-550 m., lower Coniacian-lower Santonian) contains a high ratio of fine-grained carbonates. Actually, this Fm. includes marls and marly limestones that bear ammonoids, inoceramids and planktonic foraminifera. Its maximum thickness is located W of the Villalba de Losa town and diminishes towards the SE. Towards the E, the Losas Fm. laterally passes to the Zadorra Fm. mentioned above, which was clearly deposited in deeper settings.

3rd DAY FIRST STOP

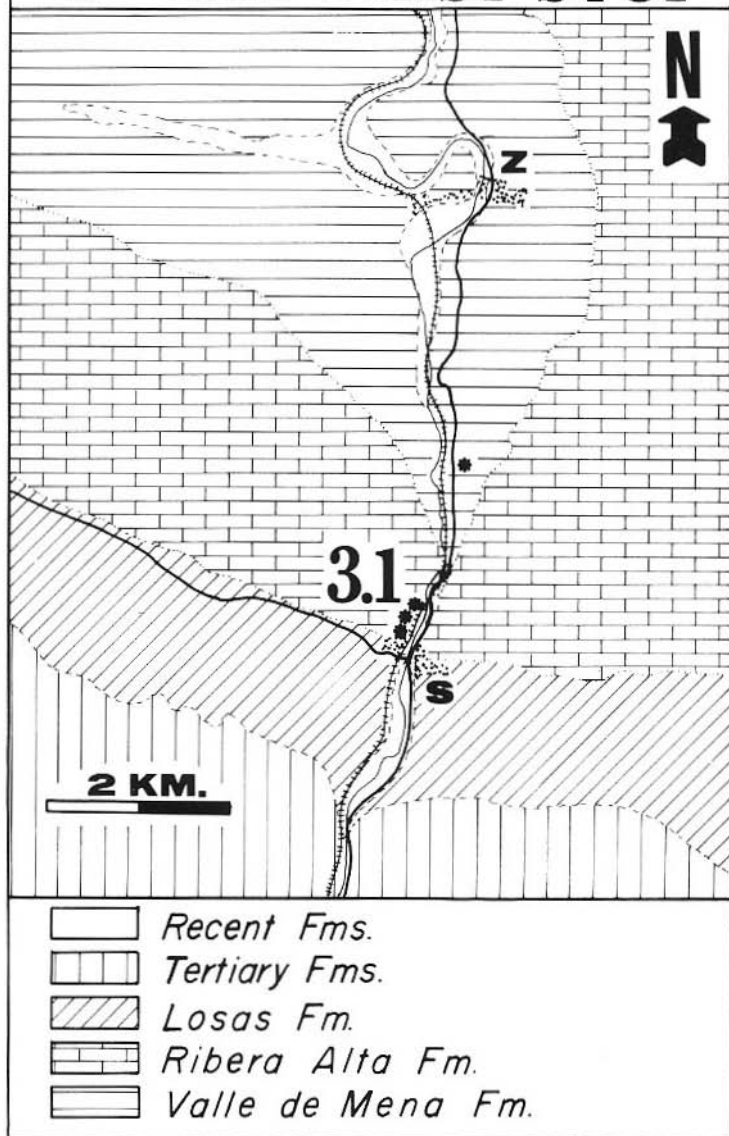


*Fig.3.1.- Geographic and geologic location of the first stop on the third day. (3.1: Subijana). Z: Zuazo de Cuartango; S: Subijana (*marks the itineraries followed).*

MORNING:

FIRST STOP (3.1): THE RIBERA ALTA FM. IN THE SUBIJANA SECTION

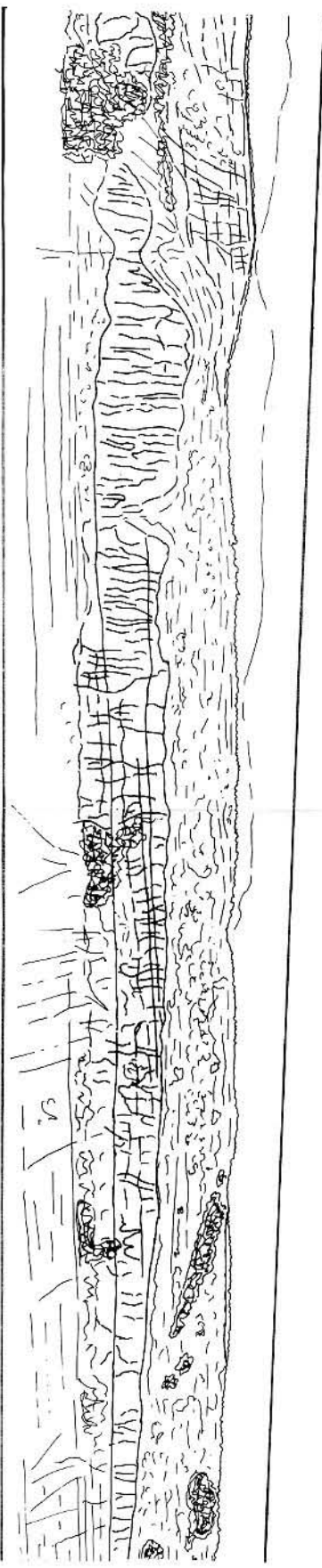
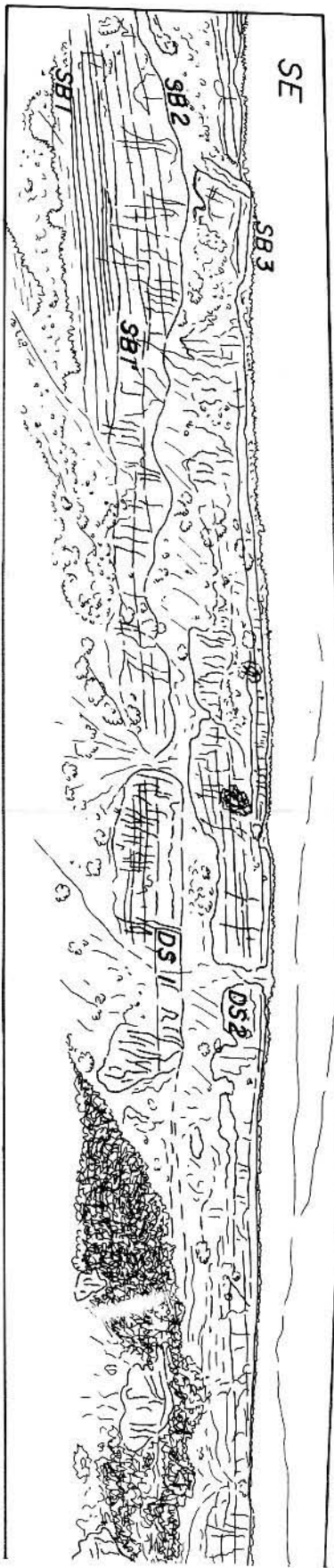
Near the Subijana village, the best exposures of the Ribera Alta Fm. can be observed along the A-68 Highway, the railway line Bilbao-Madrid and the local road (**fig. 3.1**). The largest and most spectacular silica nodules can be found in the Subijana outcrops, which are included in the facies corresponding to the platform margin located on the western side of the railway. Deeper marly sediments—typically indicative of the transition to basinal environments—are well-developed on the eastern side of the railway.

A) GENERAL LANDSCAPE AND SEQUENTIAL ANALYSIS

According to the sequential analysis employed at the beginning (**Van Wagoner et al, 1988**), we have established the existence of two depositional sequences (DS 1 and DS 2) which compound the Ribera Alta Fm. in the Subijana section. The DS 1 sequence shows the typical features of progradational mechanisms of formation. In fact, the well-developed clinoforms laterally evolve to marly limestones and marls of deeper environments (basin) towards the E and SE. **Fig.3.2** represents a general aspect of the Ribera Alta Fm. in this area, and **fig.3.3** is a detail of the transition limestone/marl just in the platform margin (Subijana section).

Unlike the widespread and tabular morphology of the carbonate bodies of the DS 1 sequence, the DS 2 seems to suggest the existence of greater offshore carbonate banks (**Wilson, 1975**) with lateral transitions to interbank (W) and basinal (E) marly deposits. Clearly, the DS 2 sequence is composed by non-continuous carbonate masses which thicken outwards and reach the maximum development just in the platform margin domain. **Fig.3.4** is an idealized scheme of the Subijana carbonate platform model and also shows the position of the main nodular chert appearances in the area. Thus, the major concentration of the nodular chert appears towards the uppermost part of the DS 1 near the Subijana village. On the other hand, this type of chert is also abundant just at the top of the DS 2 sequence outcropping close to the Artaza T.V. station, which is located very far from the area we will visit today.

SE



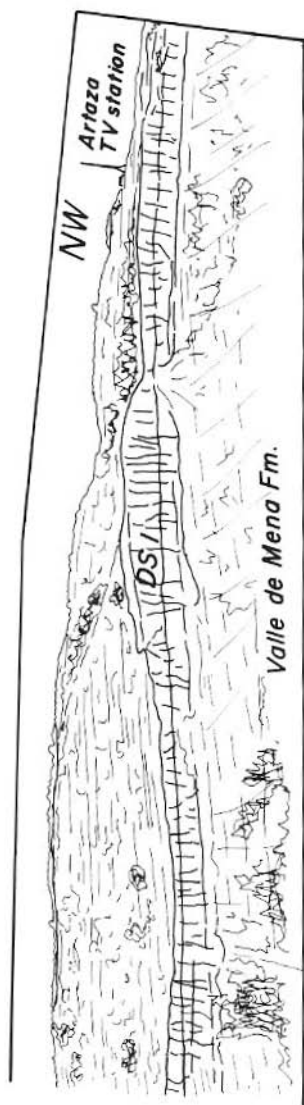


Fig.3.2.- A panoramic landscape showing the morphology of the Ribera Alta Fm. carbonate bodies in the Subijana area. Progradational clinoforms dipping a very low angle can be observed. The DS 1 and DS 2 sequences can be well identified, the latter possibly corresponds to a major carbonate bank that laterally changed to marly deposits. The total section is 4.5 km. long.

B) SILICIFICATION

A great concentration of different nodular chert types and selective replacement of *Pycnodonte* shells occurs towards the uppermost part of DS 1 sequence. We can distinguish at least three different morphologies of chert nodules, specifically, between the local road tunnel and an abandoned quarry.

1. Small nodular chert controlled by pre-existing *Thalassinoides* burrow systems. One can see a great number of nodules following the original bedding planes (**fig. 3.5 A,B,C,D**). In general, they can have a diameter of up to 10 cm. and a length of 50 cm. with a milky-white aspect and a host rock net contact.

Sometimes, we observe samples of nodular chert, which have a similar aspect, but whose disposition is oblique in respect to the original bedding planes (**fig. 3.5 C,D**).

In thin section, the selective replacement of the marine sediment that forms part of the *Thalassinoides* burrow systems is clear. Here, the silicification is constituted by micro- and cryptocrystalline quartz and fibrous varieties (chalcedonite) which infill small cavities. We appreciate ghosts of pellets, foraminifers, echinoid spines and other bioclasts, together with siliceous sponge spicules that were replaced by the microquartz mass. Individual euhedral limpid crystals of dolomite occur in the microquartz mass too.

2. Big nodular chert. Towards the top of DS 1 sequence, we observe the occurrence of individual subspherical/ovoidal chert nodules, which can reach a size of up to 20 cm. in width and 50 cm. in length, with a clear inner zonation (**fig. 3.6 A,B,C**).

From the inner part to the crust we can appreciate in **fig. 3.6 B**: (1). An irregular small zone of megaquartz crystals infilling the previous open spaces (a). In thin section, this megaquartz mass presents a polygonal texture without any evidence of anhydrite laths.

(2). A very fine and dense chert band (b), with a cream-white porcellanite aspect, is constituted by massive microquartz which contains ghosts of bioclasts.

(3). An external band of milky-white porous chert (c), with an obvious weathering like thin onion layers. In thin section, the microquartz mass is scattered with euhedral dolomite crystals. The dolomite crystals correspond to a later and limited dolomitization stage,

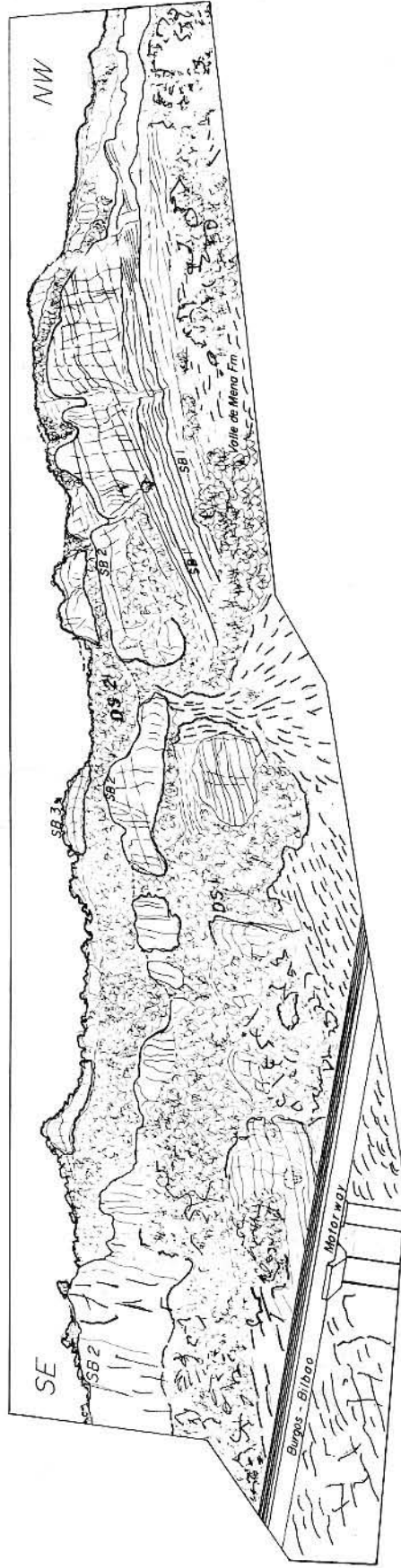


Fig.3.3.- A detail of the transition from platform margin limestones to basinal marls showing the lateral change of facies in the Subijana section by the A-68 Bilbao-Burgos highway. The increase in thickness in the DS 1 sequence to the left of the picture is only an optical effect due to the proximity to the outcrop. The total section is about 800 m. long.

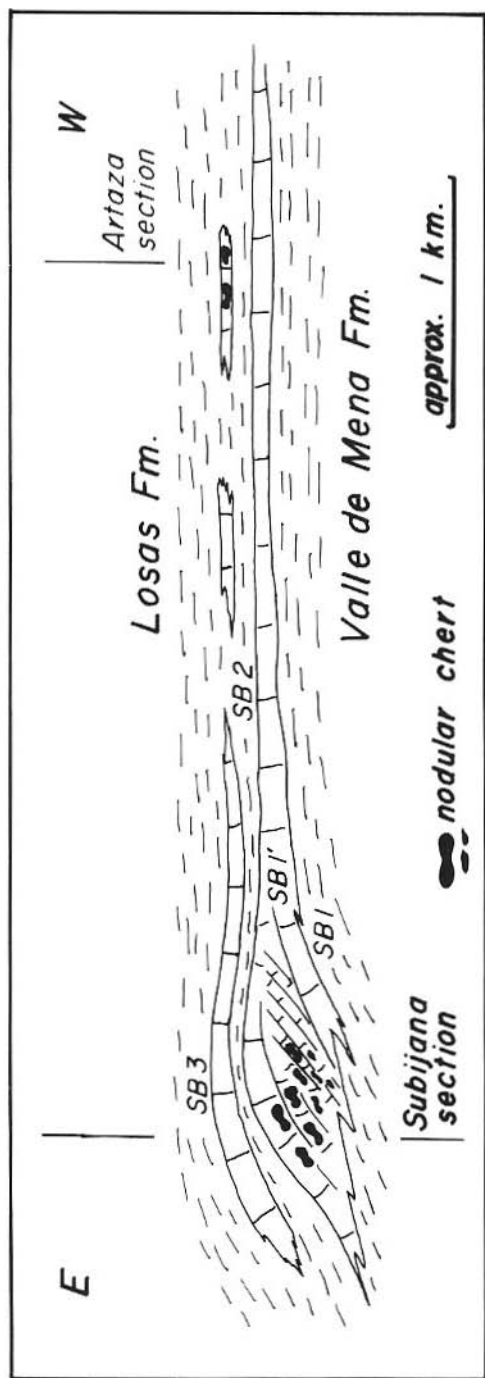


Fig.3.4.- An idealized scheme of the Ribera Alta platform in the Subijana-Artaza area. The DS 1 sequence corresponds to a widespread platform that bears the main nodular chert concentrations near the top (SB 2). The DS 2 sequence laterally passes towards the W to interbank marly deposits, and towards the E to deeper basinal marls.

which was undergone by the Ribera Alta Fm. In this case, the euhedral dolomite crystals agree with the diagenetic replacement controlled by force of crystallization suggested by **Maliva and Siever (1988 a)** in many diagenetic replacements.

3. Nodular chert with Liesegang rings. This type of nodules occurs particularly in association with small nodular chert along a few meters. They are a little bigger than the former and have a grey color which is darker than that of the host rock. The Liesegang rings can be characterized by closed dark lines, more open near the nucleous and closed near the area in contact with the host rock (**fig. 3.6 D**).

So far, we have not detected any geochemical compositional differences (microprobe analyses) between the dark rings and the inter-ring zone. Probably, the dark rings have a higher concentration of organic material, fluid inclusions, etc. than the inter-ring zone. These rings can be followed with difficulty inside the host rock, but they are still noticeable at first sight.

4. Selective replacement of oysters. Finally, on the top of the Subijana section (DS 2) there are concentrations of silicified *Pycnodonte* shells, with the same general aspect and microscopic characteristics as the ones described above in our characterization of the Cueva section.

In general, our findings do not coincide completely with the general trends (i.e., silica sources, depositional environments and timing of silicification) observed and proposed by **Maliva and Siever (1989)** in other Mesozoic to Middle Paleozoic Platform limestones. Thus, we agree with (a) an intraformational sponge spicule silica source, which is supported by a direct evidence, such as sponge spicules in the chert nodules and the host rock; (b) the existence of ghosts of pre-silicification carbonate cements. Yet, it is not clear that silicification occurred, in general, after burial to a depth sufficient for intergranular pressure solution and mechanical grain deformation of carbonate sand in a largely uncemented sediment.

The biggest difference between our findings and the general trends has to do with the fact that the nodular chert appears and is most abundant in high-energy subtidal limestones (grainstones), as opposed to there of normal marine wackestones and mudstones that were deposited at or below fair-weather wave base as pointed out by **Maliva and Siever (op. cit)**.

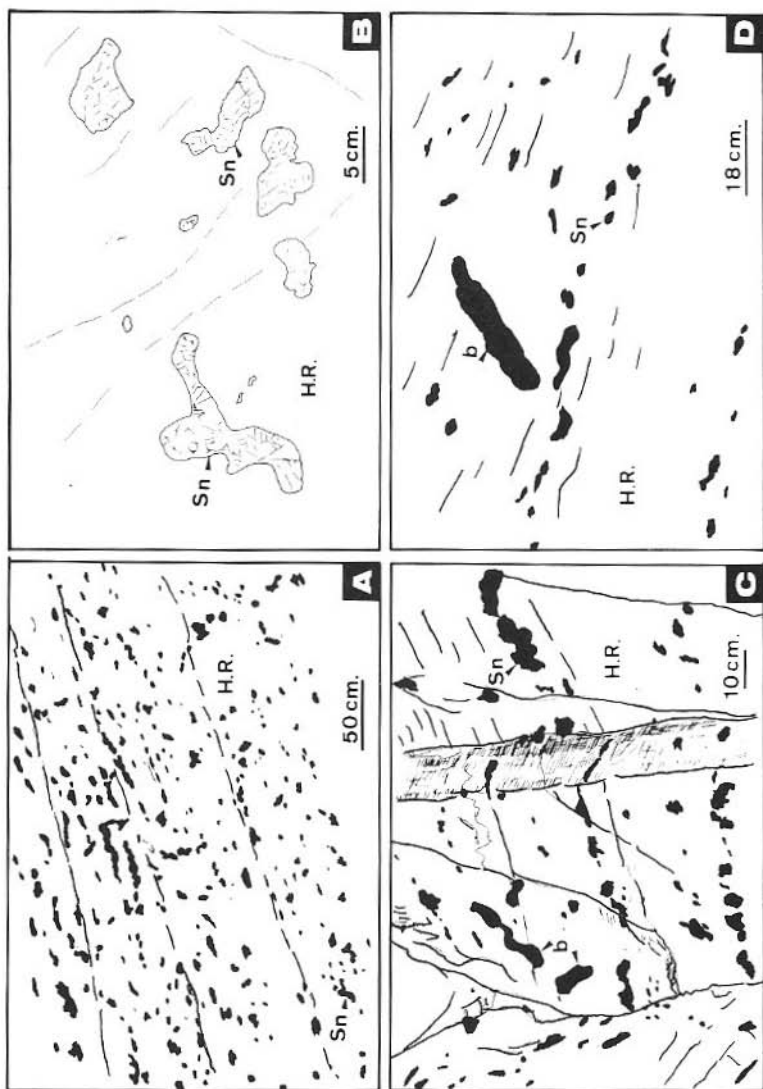


Fig. 3.5 A.- An aspect of the small nodular chert (Sn), following the original bedding planes in a bioclastic calcarenite (H.R.). **B)** A detail of A, with the typical nodular shapes (Sn) controlled by *Thalassinoides* burrow systems in a calcarenite (H.R.). **C and D)** Nodular chert (Sn) following the original bedding planes and oblique bioturbations, now as nodular chert, cross-cutting the original bedding planes.

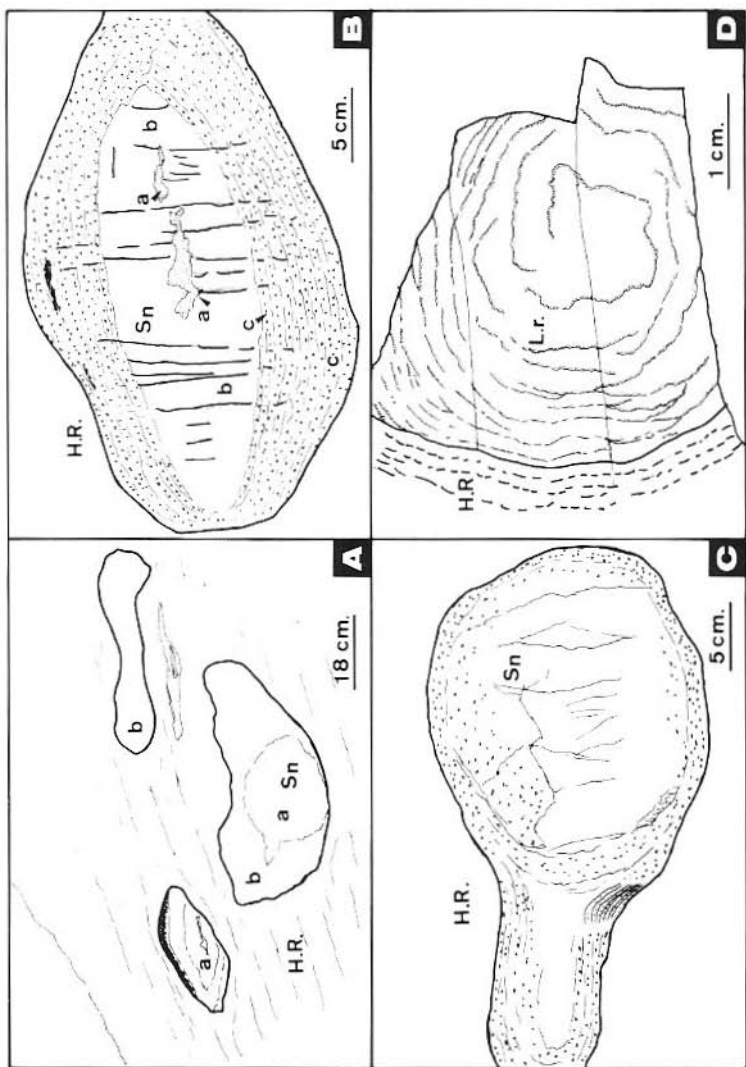


Fig.3.6. A) Ovoidal nodules of chert (Sn) with zonations (a); sometimes due to weathering, the holes are the only remains (b) in the host rock (H.R.). B) A detail of A, with a zonation of the nodular chert (Sn): (a) a zone of white megaquartz; (b) a band of fine and dense porcelaneous chert, (c) an external milky-white band with high porosity. C) Another big nodule with a clear example of weathering of the external band in onion-like layers. D) A fragment of chert nodule with Liesegang rings (L.r.) which continue towards the host rock (H.R.).

REFERENCES.

AMIOT, M. (1982)

El Cretácico superior en la Región Navarro-Cántabra. In: El Cretácico de España. Universidad Complutense. p. 88-111.

AMIOT, M.; FLOQUET, M. et MATHEY, B. (1983)

Relations entre les trois domaines de sédimentation du Crétacé Supérieur. In: Vue sur le Crétacé Basco-Cantabrique et Nord-Iberique. Mémoires Géologiques de L'Université de Dijon. p. 169-176.

ARRIORTUA, M.I.; ELORZA, J. y AMIGO, J.M. (1984)

Índices de cristalinidad y volumen de celda unidad de algunos cuarzos diagenéticos presentes en la Cuenca Vasco-Cantábrica. I Congreso Nacional de Geología. v. III, p.177-188.

BADILLO, J.M. and GARCIA-GARMILLA, F. (1985)

A tectonosedimentary episode in the «Black Flysch» of Basque-Cantabrian Basin (Northern Spain). 6th. European Regional Meeting of Sedimentology I.A.S. Lleida. Abstracts Book. p. 500-503.

BADILLO, J.M. and GARCIA-GARMILLA, F. (1989a)

The basal unconformity of the upper Albian Black Flysch: genesis and petrology (Basque Coast, Northern Spain). E.U.G. V Meeting. Terra Abstracts, vol.1, No.1, p.414-415.

BADILLO, J.M. and GARCIA-GARMILLA, F. (1989b)

Petrology of the terrigenous middle-upper Albian Series (Basque Coast, Northern Spain). 10th. I.A.S. Regional Meeting. Budapest. Abstract Book. p.5-6.

BOILLOT, G. (1981)

De la subduction a la collision: l'exemple des Pyrénées. Bull. B.R.G.M.: I (2), p.93-101.

BOILLOT, G. (1984a)

Les marges continentales stables et leur destin.
Bull. Soc. géol. France, XXVI, p.517-531.

BOILLOT, G. (1984b)

Some remarks on the continental margins in the Aquitaine and French Pyrenees. Geological Magazine, 121, p.407-412.

BOSELLINI, A. (1984)

Progradation geometries of carbonate platforms: examples from the Triassic of the Dolomites, northern Italy.
Sedimentology, 31, p.1-24.

BOYCE, A.J.; FALLICK, A.E.; HAMILTON, P.J. and ELORZA, J. (1990)

Diagenesis of celestite in quartz geodes from the Basque-Cantabric Basin, Northern Spain; Evidence from Sulphur and Strontium isotopes. Chemical Geology, v. 84 p.354-356.

BROWN, L.F. and FISHER, W.L. (1977)

Seismic-stratigraphy interpretation of depositional systems: examples from Brazil rift and pull-apart basins. in: Payton, C.E. (Ed.) Seismic Stratigraphy: Applications to Hydrocarbon Exploration, A.A.P.G. Mem.26, p.213-248.

CAMPOS, J. (1979)

Estudio geológico del Pirineo vasco al W del río Bidasoa.
Munibe 1-2: 3-139.

CHOUKROUNE, P.; SEGURET, M. et GALDEANO, A. (1973)

Caracteristiques et evolution structurale des Pyrenées: un modèle de relations entre zone orogenique et mouvement des plaques.
Bull. Soc. géol. France, XV(5-6), p.600-611.

CUEVAS, J. ; EGUILUZ, L.; RAMON-LLUCH, R. y TUBIA, J.M. (1982)

Sobre la existencia de una deformación tectónica compleja en el flanco N del sinclinal de Oiz-Punta Galea (Vizcaya): Nota preliminar. Lurralde (Investigación y Espacio) p. 47-61.

DEREGNAUCOURT, D. et BOILLOT, G.
(1982)

Structure géologique du Golfe de Gascogne.
Bulletin du B.R.G.M. (2) I.No.3. p. 149-178.

EHRMANN, W.U. (1990)

Upper Cretaceous flints in Central NW-Europe, paleoproductivity
and Milankovitch cycles. Cahiers du Quaternaire, 17, p. 77-83.

ELORZA, J.; ORUE-ETXEARRIA, X. y
LAMOLDA, M.A. (1984)

Existencia de una fracturación intensa en el área de Sopelana - Me-
ñacoz (N.E. de Bilbao). I Congreso Español de Geología.
T.III, p. 177-188.

ELORZA, J. and
RODRIGUEZ-LAZARO, J. (1984a)

Late cretaceous quartz geodes after anhydrite from Burgos, Spain.
Geological Magazine. vol. 121 (2) p. 107-113.

ELORZA, J. y
RODRIGUEZ LAZARO, J. (1984b)

Existencia de estructuras nodulosas de celestina afectadas por
silicificación en el Valle de Losa (N. de Burgos).
Estudios Geológicos. vol. 40: p. 41-48.

ELORZA, J. y ARRIORTUA, M.I. (1985)

Silicificación de fragmentos de coníferas en las arenas de la
Formación Utrillas (N.Burgos). Soc. Esp. de Miner. v. 8: 73-82.

ELORZA, J.; ARRIORTUA, M.I. y
AMIGO, J.M. (1985)

Índices de cristalinidad en los sílex de carácter turbidítico de Barrika
(NE de Bilbao). Boletín Geológico y Minero. XCVI-I: p.74-81.

ELORZA, J. and ORUE-ETXEARRIA, X. (1985)

An example of silicification in *Gryphaea* sp. shells from Laño
(South of Vitoria, Spain). 6th European Regional Meeting of Sedi-
mentology. I.A.S. Lleida. Abstracts book. p. 556-559

**ELORZA, J. and
RODRIGUEZ-LAZARO, J.(1986)**

Quartz geodes with celestite and calcite after anhydrite from Langre (Santander, Spain). In: Proceedings of the International Meeting "Geochemistry of the Earth Surface and Processes of Mineral Formation" Granada.(Ed. Rodríguez-Clemente and Tardy).
C.S.I.C. and C.N.R.S. p. 837-847

ELORZA, J. and BUSTILLO, M.A. (1989)

Early and late diagenetic chert in carbonate turbidites of the Senonian flysch, N.E. Bilbao, Spain). In: Siliceous Deposits of the Tethys and Pacific Regions. J.R. Hein and J. Obradovic Editors.
Springer-Verlag. Chapter. 7: 93-105.

ELORZA, J. and GARCIA-GARMILLA, F. (1991)

The Cueva-Bedón Carbonate Platform: Sedimentary and Petrological evidence for depositional sequences (Upper Cretaceous, Basque Cantabrian Region, Northern Spain.
12th. Regional Meeting IAS. Bergen. Abstracts book. p. 15.

ELORZA, J. and FALLICK, A.E. (in press).

Oxygen isotopic data of the early and late diagenetic chert in carbonate turbidites (Upper Cretaceous), Northeast Bilbao, Spain.
Geogaceta.

FEUILLEE, P. et RAT, P.(1971)

Structures et paléogéographies Pyrénéo-Cantabriques. In: Histoire structurale du Golfe de Gascogne. Technip. Paris, p. V.1-V.1.48.

FLOQUET, M. (1983)

La plate-forme nord-castillaine et les facies proximaux. In: Vue sur le Crétacé basco-cantabrique et nord-ibérique. Une marge et son arrière-pays, ses environnements sédimentaires.
Mém. Géol. Univ. Dijon, 9, p.141-168.

FLOQUET, M. (1991)

La Plate-forme Nord-Castillane au Crétacé Supérieur (Espagne).
Arrière-pays ibérique de la marge passive basco-cantabrique.
Sédimentation et Vic. Mém. Geol. Univ. Dijon, 14, 925 p.

FLOQUET, M.; ALONSO, A.; MELENDEZ, A.
(1982)

El Cretácico Superior en la Meseta norcastellana. In:
El Cretácico de España. Universidad Complutense, 387-453.

FLOQUET, M.; PHILIP, J.; BABINOT, J.F.;
TRONCHETTI, G. et BILOTTE, M. (1987)

Transgressions- Régressions marines et événements
biosédimentaires sur les marges Pyrénéo-Provençales et Nord-
Ibériques au Crétacé supérieur. In: Transgressions et Régressions au
Crétacé. Mémoires géologiques de l'Université de Dijon.
n° 11. p.245-258.

FOLK, R.L. (1975)

Third-part reply to Hatfield: Discussion of Jacka A.D. 1974
"Fossils by length-slow chalcedony and associated dolomitization".
Journal of Sedimentary Petrology 44: 421-427.

FOLK, R.L. and PITTMAN, J.S. (1971)

Length-slow chalcedony: a new testament for vanished evaporites.
Journal of Sedimentary Petrology. 41, 1045-1058.

FOLK, R.L. and SIEDLECKA, (1974)

The "schizohaline" environment: its sedimentary and diagenetic
fabrics as exemplified by late Paleozoic rocks of Bear Island,
Svalbard. Sedimentary Geology, 11, p.1-15.

GARCIA-GARMILLA, F. and ELORZA, J. (1991)

Sedimentary and Petrological evidence for depositional sequences
in the El Ribero carbonate platform (Upper Cretaceous, Basque-
Cantabrian Region, Northern Spain). 12th. Regional Meeting IAS.
Bergen. Abstracts book p. 20.

GREGG, J.M.; GOLDSTEIN, S.T.; and
WALTERS, Jr. L.J. (1977)

Occurrence of strained quartz in the siliceous frustules of cultured
freshwater diatoms. Journal of Sedimentary Petrology.
v. 47. p. 1623-1629.

HATFIELD, C.B. (1975)

Replacement of fossils by length-slow chalcedony and associated dolomitization (Discussion of a paper by A.D. Jacka, *J.Sed. Pet.* vol. 44, 421-427). *Journal of Sedimentary Petrology* 45, 951-952.

HUGHS, T. (1889)

On the manner of occurrence of beekite and its bearing upon the origin of siliceous beds of Paleozoic age.

Mineralog. Magazine, 8, p.265-271.

JACKA, A.D. (1974)

Replacement of fossils by length-slow chalcedony and associated dolomitization. *Journal of Sedimentary Petrology*, 44, 421-427.

JENKYN, H.C. (1980)

Cretaceous anoxic events from continents to oceans.

J. Geol. Soc. London, v. 137, p. 171-188.

KEENE, J.B. (1983)

Chalcedonic quartz and occurrence of quartzine (length-slow chalcedony) in pelagic sediments. *Sedimentology* 30: 449-454.

KITA, I.; TUGUCHI, S. and

MATSUBAYA, O. (1985)

Oxygen isotope fractionation between amorphous silica and water at 34-93°C. *Nature*, vol. 314,7, p. 83-84.

LE PICHON, X.; BONNIN, J.;

FRANCHETEAU, J. et SIBUET, J.C. (1971)

Une hypothèse d'évolution tectonique du Golfe de Gascogne. in: *Histoire Structurale du Golfe de Gascogne*, p.VI-11.1-VI-11.4.

LOHMANN, K.C. (1988)

Geochemical patterns of meteoric diagenetic systems and their application to studies of paleokarst. in: N.P. James and P.W. Choquette (Eds.) *Paleokarst*. Springer-Verlag. New York. p.58-80.

MALIVA, R.G. and SIEVER, R. (1988a)

Diagenetic replacement controlled by force of crystallization. *Geology*, v. 16, p. 688-691.

MALIVA, R.G. and SIEVER, R. (1988b)

Pre-Cenozoic nodular cherts: evidence for opal-CT precursors and direct quartz replacement.

American Journal of Science. v. 288, p. 798-809.

MALIVA, R.G. and SIEVER, R. (1989)

Chertification histories of some Late Mesozoic and Middle Paleozoic platform carbonates.

Sedimentology. 36. 907-926.

MATHEY, B. (1982)

El Cretácico superior del Arco vasco. In:

El Cretácico de España. Univ. Complutense, Madrid, p. 111-136.

MATHEY, B. (1987)

Les flyschs crétacé supérieur des Pyrénées basques.

Memoires Geologiques de L'Universite de Dijon. n° 12, 399 p.

***MEIBURG, P.; MICHALZIK, D. and
SCHMITT, R. (1984)***

Fazies-kontrollierte Halokinese am Beispiel des Diapirs Salinas de Rosío (Noedspanien). Z. dt. geol. Ges. 135, p.67-130.

MOORE, C.H. (1989)

Carbonate Diagenesis and Porosity Development

Elsevier. Amsterdam. Develop. in Sediment. No.46, 338 p.

MORTIMORE, R.N. and WOOD, C.J. (1986)

The distribution of flint in the English Chalk, with particular reference to the «Brandon Flint Series» and the high turonian flint maximum. In: The scientific study of flint and chert. Edit. G.de C. Sieveking & M.B. Hart. Cambridge University Press. 7-20.

MURATA, K. and NORMAN, M.B. (1976)

An index of Cristallinity for quartz.

American Journal of Science.v.276, p.1120-1130.

PUJALTE, V. (1982)

La evolución paleogeográfica de la cuenca «Wealdense» de Cantabria. Cuadernos de Geología Ibérica. 8, p.65-83.

RAT, P. (1959)

Les Pays Crétacés Basco-Cantabriques (Espagne). Thèse Fac. Sc. Publ. Univ. Dijon. Presses Universitaires de France. XVIII, 525 p.

RAT, P. (1982)

Subsidence et évolution des environnements sédimentaires sur la marge cantabrique (Espagne) au Crétacé.
Neues. Jb. Geol. Palaont. Abh. 165: 32-45.

RAT, P. (1983)

Les Regions Basco-Cantabriques et Nord-Iberiques: presentation, problemes poses. In: Vue sur le Crétacé Basco-Cantabrique et Nord-Iberique. Une marge et son arriere-pays, ses environnements sédimentaires. Mem. Géol. Univ. Dijon, 9. p. 1-24.

**RAT, P.; AMIOT, M.; FEUILLEE, P.;
FLOQUET, M.; MATHEY, B.; PASCAL, A. et
SALOMON, J. (1982)**

Etapas et style de l'évolution de la marge cantabrique et de son arrière-pays (Espagne). Acad. Sci. Paris. 295: 247-250.

RENARD, M. (1987)

Enregistrements geochemiques (element-traces et isotopes stables) des cycles transgression-regression par les carbonates pelagiques au Cours du Crétacé. In: Transgressions et Régressions au Crétacé. Memoires Géologiques de l'Université de Dijon. n°11.p. 125 142.

RIES, A.C. (1978)

The opening of the Bay of Biscay. A review.
Earth-Science Reviews. Vol. 14, p. 35-63.

ROSSY, M. (1988)

Contribution a l'étude du magmatisme mesozoïque du Domaine Pyreneen. These Université de Franche-Comte. n° 225, pg. 368.

SOLER Y JOSE, R. (1971)

El Jurásico marino de la Sierra de Aralar (Cuenca Cantábrica Occidental): los problemas poskimméricos. In: I Coloquio de Estratigrafía y Paleogeografía del Jurásico de España. Cuadernos de Geología Ibérica, 2, p. 509-532.

**TARRIÑO, A.; ARRIORTUA, M.I.; y
ELORZA, J. (1989)**

Estudio geológico del área de Peñacerrada (Alava): Petrografía y
Cristalografía de las silicificaciones existentes.
Eusko-Ikaskuntza. Cuadernos Sección 5, 43-135.

**URTIAGA, M.K.; ARRIORTUA, M.I.;
ELORZA, J. (1990)**

Estudio de las manifestaciones silíceas del noroeste de la provincia
de Navarra. Eusko Ikaskuntza. Cuadernos de Sección 7. p. 259-279.

**VAN WAGONER, J.C.; POSAMENTIER, H.W. ;
MITCHUM Jr., R.M.; VAIL, P.R.; SARG, J.F.;
LOUTIT, T.S. and HARDENBOL, J. (1988)**

An overview of the fundamentals of Sequence Stratigraphy and key
definitions. In: Sea-Level Changes: an Integrated Approach.
S.E.P.M. Spec.Publ. 42. p. 39-45.

**ZARRAGA, E. and
RODRIGUEZ-LAZARO, J. (1990)**

Late Cretaceous ostracode faunas from the Biscay synclorium
(Basque Arc, northern Spain).
Cour. Forsch.-Inst. Senckenberg, 123: 229-238.

**WILGUS, Ch.K.; HASTINGS, B.S.; POSAMENTIER,
H.W.; VAN WAGONER, J.C.; ROSS, Ch.A. and KEN-
DALL, Ch.G. (1988)**

Sea-Level Changes: An Integrated Approach
S.E.P.M. Spec. Publ. nº 42, 407 pp.

WILLIAMS, C.A. (1975)

Sea-floor spreading in the Bay of Biscay and its relationship to the
north Atlantic. Earth Planet. Sci. Lett. vol. 24. p. 440-456.

WILSON, J.L. (1975)

Carbonate Facies in Geologic History.
Springer Verlag. New York, 471 p.